Interactions on the Dorsal Surface of eIF4E

A thesis submitted to the University of Manchester for the degree of

Master of Philosophy

in the Faculty of Life Sciences

2010

Shirley Tait

Contents

List of Figures 6

List of Tables 6

Abbreviations 7

Abstract 10

Declaration 11

Copyright Statement 12

Acknowledgements 13

Chapter One

Introduction 14

1.1 Translation Initiation 14

1.1.1The eIF4F complex 15

1.1.2 The eIF4E binding proteins 16

1.1.3 Disorder to order transition of 4E-BP1 19

1.2. Structure of eIF4E 21

1.2.1 Structure of the murine ternary complexes 21

1.2.2 Structure of yeast eIF4E in complex with m^7GDP 21

1.2.3 Structure of the yeast ternary complex 24

1.2.4 Structure of apo human eIF4E 24

1.3. Binding of eIF4E to eIF4G 26

1.3.1 Yeast eIF4E binding to eIF4G 26

1.3.2 Importance of the N-terminal region of eIF4E for binding eIF4G 27

1.4. Binding of eIF4E to 4E-BPs 29
1.4.1 4E-BP binding site 29
1.4.2 Human eIF4E binding to 4E-BPs 29
1.4.3 Importance of the N-/C-terminal region of 4E-BPs for binding eIF4E 32

1.5. Effects of phosphorylation of 4E-BPs on binding to eIF4E 35
1.5.1 Order of phosphorylation of 4E-BPs 35
1.5.2 Phosphorylation on Ser65 causes a reduction in binding to eIF4E 35
1.5.3 Release of 4E-BPs from eIF4E 36
1.5.4 Biophysical studies of binding of phosphoproteins 37
1.5.5 Structural effects of Ser65 phosphorylation 38

1.6. Aims and Objectives 41

Chapter Two
Materials and Methods 43

2.1. Strains and Plasmids 43
2.1.1. Escherichia coli Strains 43
2.1.2. Plasmid for expression in CAG629 43

2.2. Protein Methods 44
2.2.1 SDS-PAGE 44
2.2.2 Measurement of protein concentration 44
2.2.3 Expression of recombinant eIF4E 45
2.2.4 Purification of recombinant eIF4E 46
2.2.4.1 Lysis from inclusion bodies 46
2.2.4.2 Purification on m^7-GTP sepharose resin 47
2.2.5 Preparation of eIF4E for NMR studies 47

2.3. Synthesis of Peptides 48

2.4. DNA Methods 49

2.4.1 Transformation of E. Coli cells 49

2.5. Isothermal Titration Calorimetry 51

2.5.1 The Calorimeter 51

2.5.2 Preparation of samples 51

2.5.2.1 Preparation of eIF4E 51

2.5.2.2 Preparation of peptides 52

2.5.3 Isothermal titration calorimetry conditions 52

2.6. Circular Dichroism 53

2.7 Nuclear Magnetic Resonance 54

Chapter Three

Results and Discussion 55

3.1 Purification of recombinant eIF4E 55

3.2 Influence of residues of the eIF4E binding motif of 4E-BP1 on binding to eIF4E 55

3.2.1 ITC data for peptide-eIF4E pairs and role of salt bridges in stabilising α-helical conformation 57

3.2.2 NMR indicates conformational changes between wild type and mutant peptides 61

3.3 Effect of phosphorylation of 4E-BP1on Ser65 on binding to eIF4E 63

3.3.1 ITC data for phosphopeptide-eIF4E pairs and effect of charge on stabilising a-helical conformation 63

3.3.2 NMR indicates conformational changes between wild type and phosphopeptide and differences between the complexes with eIF4E 65

3.4 CD data confirm structural differences between peptides 65

Chapter Four

Conclusions and Future Perspectives 69

References 74

word count 15,128

List of Figures

Figure 1.1 Action of 4E-BP on eIF4E. 18

Figure 1.2 Structures of two murine eIF4E/m^7GDP/peptide ternary complexes. 22

Figure 1.3 Sequence alignments of eIF4E recognition motifs from eIF4Gs and the 4E-BPs. 23

Figure 1.4 eIF4G folds into a "bracelet" around the N-terminus of eIF4E. 25

Figure 1.5 Cap binding results in structural changes and alterations in the electrostatic potential on the dorsal surface of eIF4E. 25

Figure 1.6 eIF4G and p20 share some of the same binding residues on eIF4E. 28

Figure 1.7 Electrostatic surface map for eIF4E. 30

Figure 1.8 Backbone structure of 4E-$BP1_{51-67}$. 33

Figure 1.9 Effects of phosphorylation of Ser 65 on the interaction with eIF4E. 40

Figure 2.1 Schematic diagram of pCYTEXP3 plasmid. 44

Figure 3.1 Elutions of eIF4E from m^7GTP sepharose resin. 56

Figure 3.2 ITC plots for 4E-$BP1_{51-67}$ peptides binding to eIF4E. 59

Figure 3.3 NMR spectra of 4E-$BP1_{51-67}$ peptides. 62

Figure 3.4 ITC plots for phosphopeptide binding to eIF4E. 64

Figure 3.5 NMR spectra of 4E-$BP1_{51-67}$ peptides titrated with eIF4E. 66

Figure 3.6 CD spectra of wildtype peptide and K57E peptide. 67

Figure 4.1 Model of disorder-order transition. 70

List of Tables

Table 2.1 Sequences of peptides used in this study. 50

Table 3.1 Dissociation constants for peptides binding to eIF4E. 58

Abbreviations

BCA	bicinchoninic acid
BSA	bovine serum albumin
C	Centigrade
Cal	Calorie
CD	Circular Dichroism
cm	centimetre
Da	Dalton
deg	degrees
DMSO	dimethylsulphoxide
DNA	deoxyribonucleic acid
DTT	dithiothreitol
EDT	1,2-ethanedithiol
EDTA	ethylene diamine tetraacetate
eIF	eukaryotic translation initiation factor
4E-BP	eIF4E binding protein
F-moc	9-Fluorenylmethoxycarbonyl
g	gram
GDP	guanidine diphosphate
GTP	guanidine triphosphate
HEPES	N[2-hydroxyethyl]piperazine-N'-[2-ethanesulphonic acid]
HSQC	Heteronuclear Single Quantum Correlation
ITC	Isothermal Titration Calorimetry
KCl	potassium chloride
kDa	kiloDalton
KOH	potassium hydroxide
l	litre
LB	Luria-Bertani broth

MALDI-TOF	Matrix-Assisted Laser Desorption/Ionization-Time of Flight
µ	micro
m	milli
M	molar
min	minute
mm	millimetre
mRNA	messenger RNA
MWCO	molecular weight cut off
m^7GDP	7-methyl guanidine diphosphate
m^7GTP	7-methyl guanidine triphosphate
nm	nanometre
NMR	Nuclear Magnetic Resonance
OD	optical density
PABP	poly A binding protein
PAGE	polyacrylamide gel electrophoresis
PHAS-I	phosphorylated heat and acid stable protein, regulated by insulin
PMSF	phenylmethanesulphonylflouride
ppm	parts per million
RNA	ribonucleic acid
rpm	revolutions per minute
s	second
S	Svedberg
SDS	sodium dodecyl sulphate
SPR	Surface Plasmon Resonance
TFA	trifluoroacetic acid
TFE	trifluoroethanol
TIS	triisopropylsilane
Tris	tris(hydroxymethylaminomethane)
$tRNA_i^{Met}$	initiator methionyl transfer RNA

UV	ultraviolet

Amino Acid abbreviations

Ala	A	Alanine
Arg	R	Arginine
Asn	N	Asparagine
Asp	D	Aspartic acid
Cys	C	Cysteine
Gln	Q	Glutamine
Glu	E	Glutamic acid
Gly	G	Glycine
His	H	Histidine
Ile	I	Isoleucine
Leu	L	Leucine
Lys	K	Lysine
Met	M	Methionine
Phe	F	Phenylalanine
Pro	P	Proline
Ser	S	Serine
Thr	T	Threonine
Trp	W	Tryptophan
Tyr	Y	Tyrosine
Val	V	Valine

Abstract

Eukaryotic initiation factor 4E (eIF4E) is the messenger RNA cap binding protein, which recruits eIF4G and eIF4A allowing translation initiation to proceed. The eIF4E binding proteins (4E-BPs) are small, heat-stable proteins (~12KDa) that act as repressors of translation. They function by binding the same site as eIF4G on the dorsal region of eIF4E, opposite the cap binding site, thereby competing for the site with eIF4G and inhibiting translation. Phosphorylation of the 4E-BPs in response to growth factors, hormones, mitogens and cytokines causes a reduction in binding to eIF4E, allowing eIF4G to bind and translation initiation to proceed. eIF4E binding protein 1 (4E-BP1) has been shown to be unstructured in solution and folds into a helical conformation on binding eIF4E, but what predisposes the 4E-BP1 to fold in the correct conformation on the dorsal surface of eIF4E?

A number of residues of both eIF4E and 4E-BP1 have been identified which are thought to be important in the interaction between the proteins. However the role of solvent facing residues asparagine 55, lysine 57, glutamic acid 61 and arginine 63 in the α-helical stretch of the eIF4E binding motif of 4E-BP1 that are not directly involved in binding eIF4E was still unexplained.

In this study a number of techniques have been employed to try and further our understanding of the role of folding in determining the affinity between 4E-BP1 and the dorsal face of eIF4E and thus the ability of 4E-BP1 to act as an inhibitor of translation. Isothermal titration calorimetry was used to determine binding affinities between peptides of $4E\text{-}BP1_{51\text{-}67}$ and recombinant eIF4E along with circular dichroism and NMR studies on the peptides in solution and titrated with recombinant eIF4E. These residues were identified as contributing to the propensity of the 4E-BP1 to fold into the correct conformation for binding to eIF4E.

So how does phosphorylation of 4E-BP1 cause a reduction in binding to eIF4E? A number of possibilities have been put forward. One explanation is that phosphorylation of 4E-BP1 could lead to electrostatic repulsion against a glutamic acid residue on eIF4E and cause release of 4E-BP1 from eIF4E, thereby allowing eIF4G to bind and translation initiation to proceed. Another possibility is that the close proximity of the phosphorylated serine on 4E-BP1 to this glutamic acid on eIF4E and glutamic acid 61 of the 4E-BP1 itself could lead to destabilisation of the α-helix within the binding motif. However the role of phosphorylation of the 4E-BPs in terms of structural effects on the region of their eIF4E binding motif has remained uncharacterised.

Isothermal titration calorimetry and NMR experiments in this study indicate that phosphorylation of serine 65 at the C-terminal end of the helical region of 4E-BP1 can affect the disorder-order transition to favour the unfolded form that cannot bind eIF4E. This adds to the growing data on unstructured proteins and can give insight into the mechanisms employed by this group of proteins.

Declaration

No portion of the work referred to in the thesis has been submitted in support of an application for another degree or qualification of this or any other university or other institute of learning

A major part of the work presented in this thesis has been accepted for publication:

Shirley Tait, Kaushik Dutta, David Cowburn, Jim Warwicker, Andrew J. Doig and John E.G. McCarthy (2010) Local control of a disorder-order transition in 4E-BP1 underpins regulation of translation via eIF4E *Proc. Natl. Acad. Sci. USA*

Copyright Statement

Acknowledgements

First I would like to thank my supervisor Professor John McCarthy for allowing me the time and resources to perform this work, while continuing as a research technician in his lab. I am grateful for the opportunity.

Many thanks also to members of the McCarthy group, past and present, for generating a friendly, lively and interesting workplace for the last ten years. I have learnt a great deal from numerous members of the lab and I have been lucky to have been with this group for so long. In particular, thanks to Dr Abigail Stevenson for reading the manuscript.

For training and advice regarding the calorimetry experiments, I thank Dr Sanjay Nilapwar. Thanks also to Professor Andrew Doig for collaborating with the CD experiments and Marina Golovanova and Dr Chris Storey for technical assistance with the peptide synthesis and mass spectrometry respectively.

Further acknowledgements must go to our collaborators in the New York Structural Biology Centre. To Professor David Cowburn, for allowing me the courtesy of visiting the facility in New York and Dr Kaushik Dutta, who performed the NMR experiments and generously gave his time to show me the machines in use and how the samples are prepared.

Finally thanks to the University of Manchester staff training and development unit for financial assistance.

Chapter One

Introduction

1.1 Translation Initiation

Protein synthesis in eukaryotes is a complex process consisting of three stages: initiation, elongation and termination. Initiation is the step where eukaryotic translation initiation factors (eIFs) aid the ribosome to bind a messenger RNA (mRNA) and an initiator methionyl transfer RNA ($tRNA_i^{Met}$) is placed at the start codon.

Translation initiation begins with the separation of the 80S ribosome into 60S and 40S subunits. eIF1, eIF1A, eIF3 and eIF5 all bind the 40S subunit. These factors have a number of functions and can form multiprotein complexes binding to the ribosome in a stepwise manner. A ternary complex consisting of eIF2/GTP/$tRNA_i^{Met}$ then joins the 40S subunit to form the 43S complex, mediated by eIF1, eIF1A, eIF3 and eIF5, which form a multifactor complex that plays a role in binding the 40S subunit and promoting formation of the 43S complex. In order for the 43S complex to bind an mRNA it requires the eIF4F complex, which aids its binding to the 5' cap structure m^7GpppN on the mRNA (where N is the first nucleotide of the mRNA). The 43S complex binds the mRNA to form the 48S complex and scans along to the AUG start codon. Once the start codon is reached the initiator methionyl tRNA is positioned and GTP hydrolysed by eIF5. eIF1, 1A, 2, 3 and 5 are released, and eIF5B aids the joining of the 60S subunit with the 40S to form the 80S initiation complex and elongation can proceed. For some recent reviews of the factors involved, see Algire and Lorsch, 2006 (start codon recognition); Hinnebusch, 2006 (eIF3); Mitchell and Lorsch, 2008

(eIF1 and 1A). The initiation stage provides key targets for regulation of translation and is an important step for control of protein synthesis.

1.1.1 The eIF4F complex

In mammals the eIF4F complex comprises the initiation factors eIF4E, eIF4G and eIF4A. A novel cap binding protein was identified by Sonenberg and colleagues in 1978 and was first purified by affinity chromatography on sepharose coupled m^7GDP (Sonenberg *et al*, 1979). This novel protein is now known as eIF4E and binds to the 5' cap structure on mRNA. eIF4G binds eIF4E, and acts as a scaffold for other proteins, including eIF4A, eIF3 and the poly-A binding protein (PABP), providing a link between the mRNA and the ribosome. eIF4A has RNA-dependent ATPase activity and, along with eIF4B, acts as an RNA helicase to unwind secondary structures within the mRNA (reviewed in Gingras, Raught and Sonenberg, 1999).

Due to its pivotal role in the translation initiation pathway eIF4E is an important target in the regulation of translation. It is the least abundant of the initiation factors and is the rate limiting factor in the eIF4F complex (Hiremath *et al*, 1985). Regulation of eIF4E activity is on a number of levels: by increasing eIF4E mRNA expression; by phosphorylation; and by translational inhibitors called the eIF4E-binding proteins (4E-BPs). Volpon *et al* (2010) have recently shown the molecular basis of inhibition of a further class of inhibitors, the really interesting new gene (RING) domain containing proteins. eIF4E is phosphorylated in response to extracellular stimuli such as growth factors, hormones, mitogens and cytokines and generally correlates with increased translation rate and cell growth. For example, heat shock of HeLa cells caused a decrease in phosphorylation of eIF4E with a repression of protein synthesis (Duncan *et al*, 1987). Ser209 has been identified as the phosphorylation site and is phosphorylated by MNK1 (MAP kinase interacting protein kinase 1), which is a target

for ERK and p38 MAP kinases (reviewed in Sonenberg and Gingras, 1998; Gingras, Raught and Sonenberg, 1999; Raught and Gingras, 1999). Two models have been proposed for the role of phosphorylation of eIF4E in translation initiation (Scheper and Proud, 2002). In the first model, eIF4E binds to the cap and is phosphorylated after assembly of the initiation complex. eIF4E is released from the cap and the 48S complex continues scanning. A second eIF4E molecule and initiation complex can then bind to the cap, speeding up ribosome loading and initiation of protein synthesis of the same mRNA. The second model proposes phosphorylation occurs later in the process after scanning is complete and the start codon recognised. This could contribute to the release of the factors, which are then free to be used in translation of a second mRNA. Which model is used depends on the pool of mRNAs needing to be translated and the availability of active MNK1. More experimental evidence is needed to confirm these models. For a recent review of the role of eIF4E in gene expression see von der Haar *et al* (2004).

Overexpression of eIF4E is found in a number of cancers, including breast, head and neck, colorectal, bladder, prostate, lung, cervical and non-Hodgkin's lymphomas (reviewed in De Benedetti and Graff, 2004). High levels of eIF4E (in the eIF4F complex) correlate with increases in the translation of proto-oncogenes and other growth factor mRNAs involved in transformation and malignancy and eIF4E may therefore be a therapeutic target for cancer treatment.

1.1.2 The eIF4E binding proteins

The eIF4E binding proteins are small, heat-stable proteins (~12KDa) that act as repressors of translation (Pause *et al*, 1994). They function by binding the same site as eIF4G on the dorsal region of eIF4E (Mader *et al*, 1995), opposite the cap binding site, thereby competing for the

site with eIF4G and inhibiting translation (Haghighat *et al,* 1995; see Figure 1.1 panel A). Phosphorylation of the 4E-BPs in response to growth factors, hormones, mitogens and cytokines causes a reduction in binding to eIF4E (Lin *et al*, 1994; Pause *et al*, 1994), allowing eIF4G to bind and translation initiation to proceed. Phosphorylation of 4E-BP1 is a two stage process, involving the FRAP/mTOR pathway, which phosphorylates two sites on 4E-BP1, acting as a priming event for further phosphorylation involving the PI3K-Akt pathway (Gingras *et al*, 1999).

Three eIF4E binding proteins have been identified in mammals: 4E-BP1 and 4E-BP2, whose protein sequences are 56% identical (Pause *et al*, 1994), and 4E-BP3, sharing 57% and 59% identity with 4E-BP1 and 4E-BP2, respectively (Poulin *et al*, 1998). Although present in most tissues, 4E-BP1 expression is highest in adipose tissue, pancreas and skeletal muscle, with expression of 4E-BP2 seemingly ubiquitous, having no preference for any tissue (Tsukiyama-Kohara *et al*, 1996). 4E-BP3 expression is highest in skeletal muscle, heart, kidney and pancreas (Poulin *et al*, 1998). The authors suggest this overlapping of expression of the 4E-BPs could be a safeguard mechanism, compensating in the event of a reduction in 4E-BP1 expression. Of the three 4E-BPs, it has been shown by affinity chromatography and surface plasmon resonance (SPR) data that 4E-BP2 has the highest binding affinity with both cap-bound and free eIF4E (Ptushkina *et al*, 1999; Abiko *et al*, 2007). The sequence of human 4E-BP1 is shown in Figure 1.1 panel B, highlighting the eIF4E binding motif, which contains the consensus sequence YXXXXLϕ, where X is a variable amino acid and ϕ is a hydrophobic residue.

A

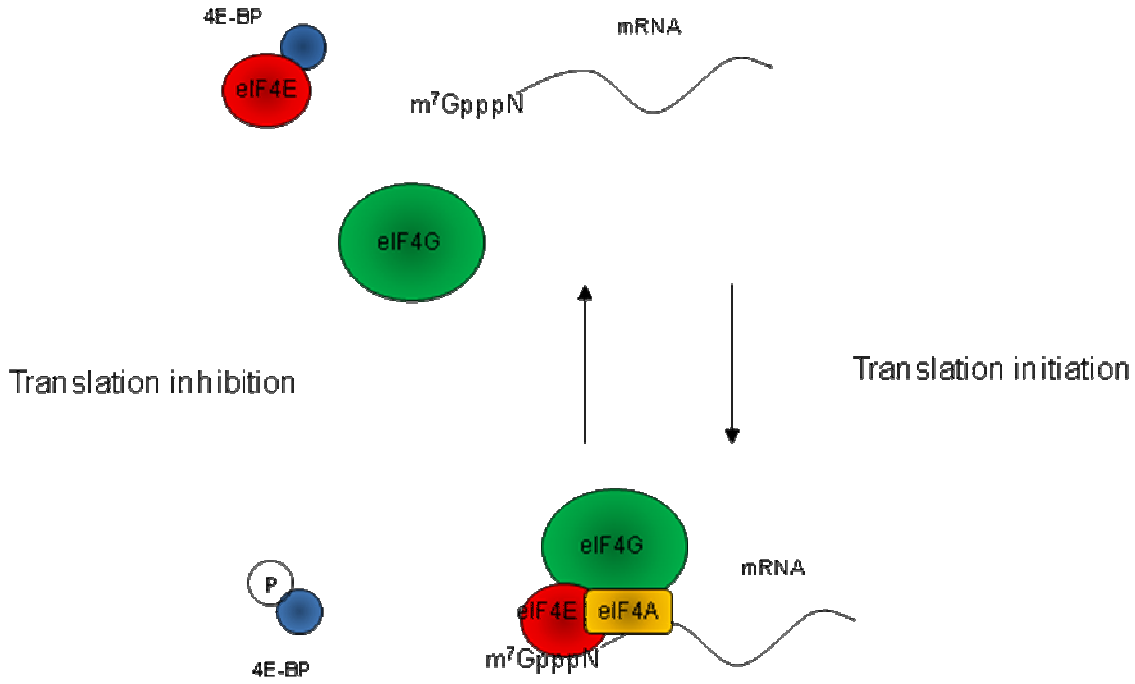

B

MSGGSSCSQT PSRAIPATRR VVLGDGVQLP PGDYSTTPGG TLFSTTPGGT RIIYDRKFLM

ECRNSPVTKT PPRDLPTIPG VTSPSSDEPP MEASQSHLRN SPEDKRAGGE ESQFEMDI

Figure 1.1 Action of 4E-BP on eIF4E.

(A) Schematic diagram of the action of the 4E-BPs on eIF4E. Phosphorylation of the 4E-BPs causes a reduction in binding to eIF4E, allowing eIF4G to bind and translation initiation to proceed. (B) Sequence of human 4E-BP1 showing the region containing the eIF4E binding motif (in dark red).

1.1.3 Disorder to order transition of 4E-BP1

4E-BP1 is one of over 100 unstructured proteins that have been identified in the Protein Database Bank (Dunker *et al*, 2002; Uversky 2002). A number of papers have been published which identify common characteristics between these proteins (see Uversky *et al*, 2000; Uversky 2002). Features of intrinsically unstructured proteins include a low content of hydrophobic residues, high net charge and low complexity of amino acid residues. Unstructured proteins are found to have a wide variety of functions (see Dunker 2002; Dyson and Wright 2002; Dyson and Wright 2005; Wright and Dyson 1999). As well as functioning as flexible linkers or spacers, they are also involved in molecular recognition and assembly, modification of proteins, as storage proteins and regulation of large multiprotein complexes. They function in a number of important cellular processes including phosphorylation, signal transduction and regulation of transcription and translation.

Unstructured proteins can infer a number of advantages such as being able to bind multiple partners, having large interaction surfaces, giving high specificity with low affinity and faster rates of association/dissociation (Dunker *et al*, 2002; Tompa 2002). Gunasekaran and colleagues (2003) argue however that some stable (native) proteins can also fulfil these roles, and that another advantage is that unstructured proteins allow large interaction surfaces to be achieved with comparatively small protein sizes. This may help mitigate against molecular crowding *in vivo*.

Unstructured proteins have the ability to undergo disorder to order transitions upon binding their partners and there are a number of folding states during this transition: random coil (unstructured); premolten globule (which has significant secondary structure but lacks tertiary structure); molten globule (which has most of the secondary structure but lacks defined tertiary structure); and ordered (native) (Gunasekaran *et al*, 2003). Uversky (2002) defined

this model as the “protein quartet” and describes protein function arising from these conformations and transitions between them. Disorder does not necessarily create the function of the protein, but the “binding and shift in the equilibrium takes care of the function” (Gunasekaran *et al*, 2003). For this reason, Tompa (2002) has described disordered proteins as “pliable” rather than unstructured.

Fletcher *et al* (1998) used ^{15}N-labelled 4E-BP1/BP2 in nuclear magnetic resonance (NMR) studies to show that 4E-BPs are unstructured in solution. The NMR spectrum showed changes on addition of eIF4E, which indicates binding, but they concluded the 4E-BPs remain largely unfolded on binding eIF4E. In further NMR studies, Fletcher and Wagner (1998) used ^{1}H, ^{13}C, ^{15}N labelled human 4E-BP1 and found there was a high degree of flexibility, with no local structure, in the absence of eIF4E. However, they could not determine the sequence order of the region between residues 56-65, which includes the binding domain. They describe the binding of eIF4E as an induced fit to the disordered 4E-BP1.

Marcotrigiano *et al* (1999) used circular dichroism (CD) spectroscopy to show 4E-BP1 has minimal secondary structure in the absence of eIF4E. In the ternary complex crystal structure with eIF4E/m^{7}GDP the region of 4E-BP1 bound to eIF4E is 50% α-helical. Alone, both recombinant full length 4E-BP1 and the 4E-BP1$_{51\text{-}67}$ peptide are largely random coil. In other words, the binding motif of 4E-BP1 undergoes a disorder to order transition upon binding eIF4E.

1.2. Structure of eIF4E

1.2.1 Structure of the murine ternary complexes

Marcotrigiano *et al* (1997) solved the crystal structure of murine $eIF4E_{28-217}$ in complex with m^7GDP and, in later studies, with peptides of mammalian eIF4GII and 4E-BP1 (Marcotrigiano *et al*, 1999). The secondary structure of eIF4E contained an 8-stranded antiparallel β-sheet, with one short and three long α-helices, with the long helices lying along the top of the β-sheet. The eIF4GII and 4E-BP1 peptides form an L-shaped structure that interacts with the α-helices along the convex dorsal surface of the eIF4E (see Figure 1.2).

The 4E-BP1 peptide adopts a similar conformation, and binds the same region as the eIF4GII peptide involving contacts that use common amino acids in the consensus binding regions (see Figure 1.3). In particular, many of the eIF4E residues making contact with the tyr, leu or the hydrophobic residue of the consensus region of the binding motif, are conserved.

1.2.2 Structure of yeast eIF4E in complex with m^7GDP

Matsuo *et al* (1997) solved the structure of yeast eIF4E in complex with m^7GDP using NMR. The structure is similar to the murine eIF4E, having an 8-stranded β-sheet with three long α-helices on the convex dorsal face and three shorter helices linking the β-sheet. The authors describe it as similar to a baseball glove with the β-sheet forming the hand and the helices being the fingers of the glove on the convex surface.

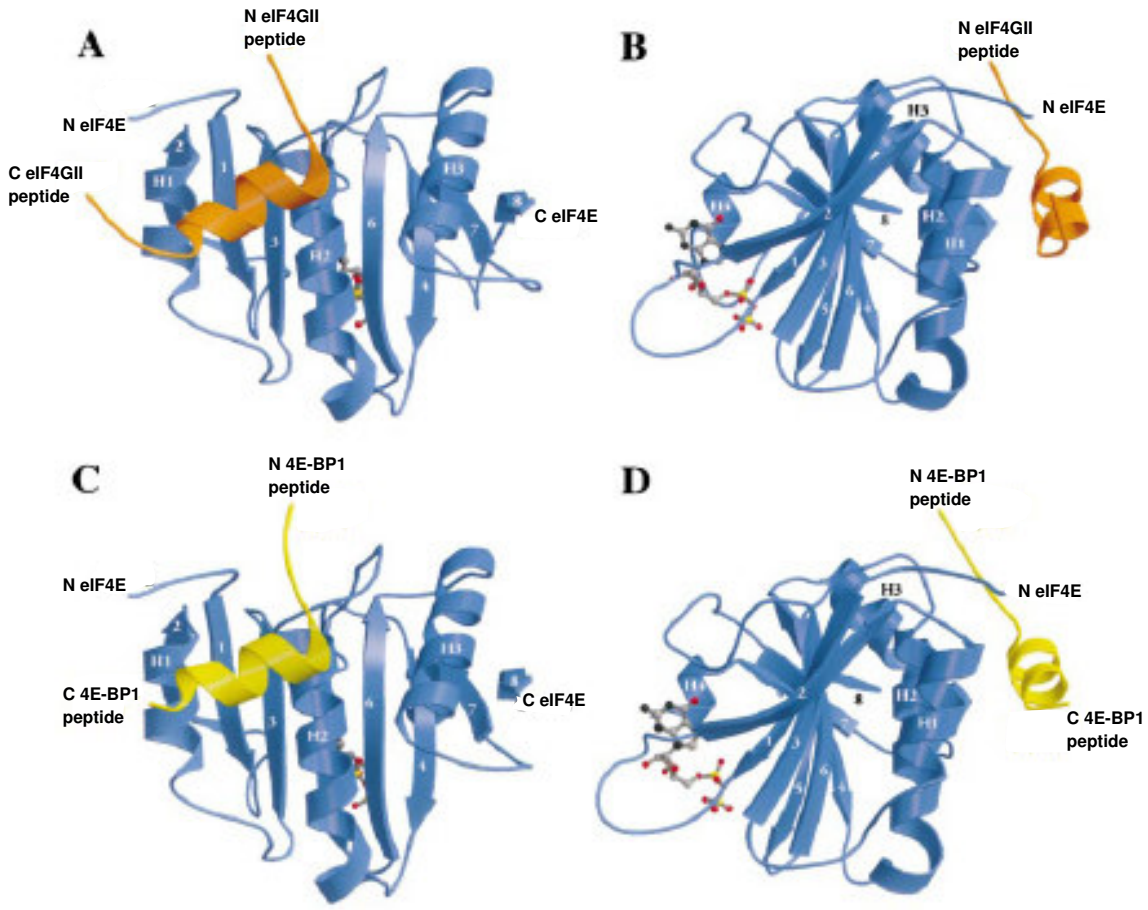

Figure 1.2 Structures of two murine eIF4E/m^{7}GDP/peptide ternary complexes.

Ribbon diagrams of murine eIF4E/m^{7}GDP/peptide ternary complexes. Views A and C are perpendicular to the eIF4E's β-sheet. Views B and D are rotated 90^O about the vertical. eIF4E is depicted in blue; the orange ribbon is the eIF4GII peptide; the yellow ribbon is the 4E-BP1 peptide; m^{7}GDP is depicted as ball and stick. eIF4GII and 4E-BP1 peptides adopt similar conformations on binding eIF4E. From Marcotrigiano *et al* (1999).

Position	-3	-2	-1	0	1	2	3	4	5	6	7	8	9	10	11	12	13
Consensus	X	X	X	**Y**	X	X	X	X	**L**	**Φ**	X	X	X	X	X	X	X
Mammalian																	
4E-BP1	R	I	I	**Y**	D	R	K	F	**L**	**M**	E	C	R	N	S	P	V
4E-BP2	R	I	I	**Y**	D	R	K	F	**L**	**L**	D	R	R	N	S	P	M
4E-BP3	R	I	I	**Y**	D	R	K	F	**L**	**L**	E	C	K	N	S	P	I
eIF4GI	K	K	R	**Y**	D	R	E	F	**L**	**L**	G	F	Q	F	I	F	A
eIF4GII	K	K	Q	**Y**	D	R	E	F	**L**	**L**	D	F	Q	F	M	P	A
Yeast																	
p150	K	Y	T	**Y**	G	P	T	F	**L**	**L**	Q	F	K	D	K	L	N
p130	K	Y	T	**Y**	G	P	T	F	**L**	**L**	Q	F	K	D	K	L	K
p20	M	I	K	**Y**	T	I	D	E	**L**	**F**	Q	L	K	P	L	S	T

Figure 1.3 Sequence alignments of eIF4E recognition motifs from eIF4Gs and the 4E-BPs.

Sequence alignments of the eIF4E recognition motifs of mammalian 4E-BP1, 4E-BP2, 4E-BP3, mammalian eIF4GI, eIF4GII, yeast p150, yeast p130 and yeast p20. Residues in red are conserved residues. Residues in the consensus sequence are numbered with respect to the invariant tyrosine (position 0). Bold residues here are invariant/conserved residues (ϕ is a conserved hydrophobic residue). X is a variable residue. Adapted from Marcotrigiano *et al* (1999).

1.2.3 Structure of the yeast ternary complex

Gross *et al* (2003) solved the NMR structure of the ternary complex of yeast eIF4E/m^7GDP/$eIF4GI_{393-490}$. On binding eIF4E, $eIF4GI_{393-490}$ forms a ring shape structure, described by the authors as a "molecular bracelet", that folds around the N-terminus of the eIF4E (see Figure 1.4). This is in agreement with NMR studies of Hershey *et al* (1999), who showed that a ^{15}N-labelled $eIF4GI_{393-490}$ fragment was unstructured in the absence of eIF4E and became folded in the presence of eIF4E. The bracelet consists of five α-helical segments and the eIF4E binding motif consensus sequence is found in the fourth helix.

Some of the main contacts involve the hydrophobic residues on the inner region of the eIF4GI bracelet, including tyr454, phe458 and phe462 on the consensus helix, which form contacts with conserved his37 and pro38 residues, or consensus hydrophobic residues val35 and phe33 in the N-terminal region of the eIF4E. Phe462 also contacts val71 and trp75 on the convex dorsal face of eIF4E (see Figure 1.4). These contacts are similar to those described by Marcotrigiano *et al* (1999) for the murine ternary complex (see Figure 1.3).

1.2.4 Structure of apo human eIF4E

Yeast studies showed eIF4E as a cupped hand "baseball glove" shape (Matsuo *et al*, 1997). These studies were done with cap bound eIF4E. Volpon *et al* (2006) studied the structure of apo (unbound) and cap/eIF4G bound human eIF4E using NMR and CD spectra. They found the apo eIF4E existed in a folded structure, describing it as an "open hand" rather than a cupped hand, with 8-stranded antiparallel strands and three long helices on the convex face.

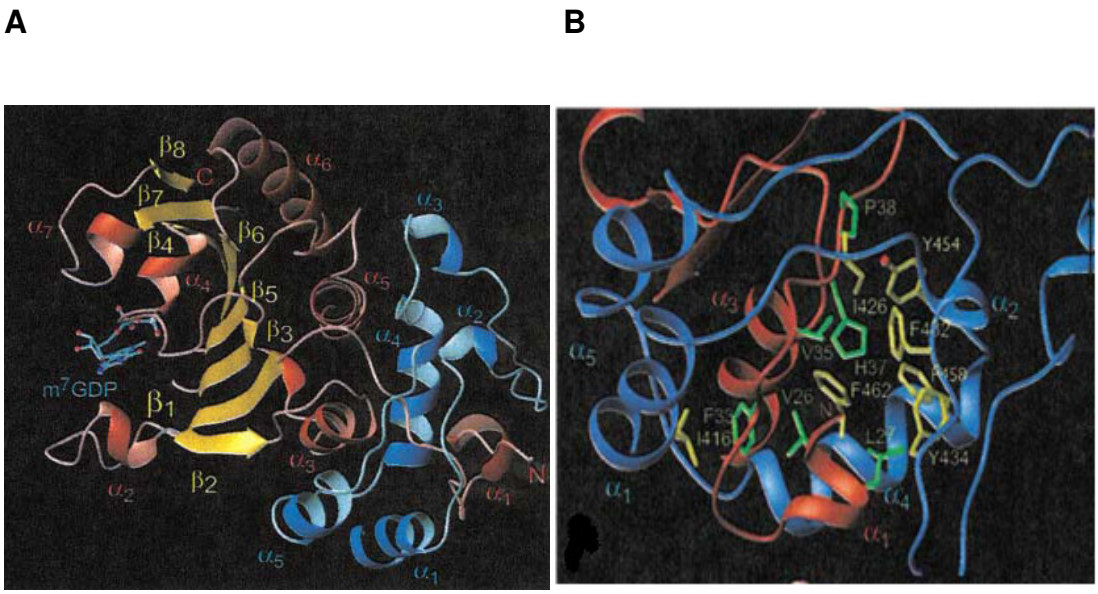

Figure 1.4 eIF4G folds into a "bracelet" around the N-terminus of eIF4E.

(A) Ribbon diagram of eIF4GI$_{393\text{-}490}$ (in blue) in complex with eIF4E (red and yellow). (B) Intermolecular contacts between eIF4GI$_{393\text{-}490}$ (in blue) and eIF4E (red). View of the dorsal surface of eIF4E showing conserved residues from the N terminus (in green) interacting with residues on the inner region of the bracelet formed by eIF4GI$_{393\text{-}490}$ (in yellow). From Gross *et al* (2003).

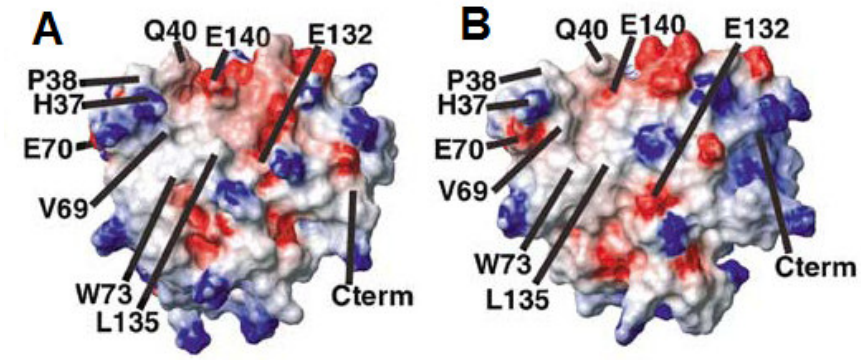

Figure 1.5 Cap binding results in structural changes and alterations in the electrostatic potential on the dorsal surface of eIF4E.

Space filling model showing the change in electrostatic potential, and important residue changes, on the eIF4E dorsal surface upon cap binding. (A) apo (unbound) eIF4E (B) cap bound eIF4E. From Volpon *et al* (2006).

The apo structure differed at the cap binding surface and the dorsal surface, with cap binding resulting in structural changes and alterations in the electrostatic potential on the dorsal surface (see Figure 1.5). eIF4G binding also resulted in changes in the cap binding region as well as the dorsal face.

1.3. Binding of eIF4E to eIF4G

1.3.1 Yeast eIF4E binding to eIF4G

Ptushkina *et al* (1998) used SPR and affinity chromatography to investigate the binding of the yeast eIF4E to eIF4G and the yeast eIF4E-binding protein, p20.

Yeast eIF4E was bound to m^7GDP resin and then incubated with 4G-BD4E (the eIF4G binding domain of eIF4E) or p20. eIF4E was then eluted with m^7GDP. There was a lower amount of eIF4E in the eluted fractions incubated with 4G-BD4E and, to a lesser extent, p20 compared with wild type (no ligands), indicating stronger binding to the cap resin in the presence of the 4G-BD4E and p20.

To look at the role of surface residues in binding, monoclonal antibodies were generated against eIF4E. These antibodies were used in affinity chromatography studies to see if they affected interaction of eIF4E with eIF4G and/or the cap structure. The authors found some antibodies that affected binding of eIF4G with eIF4E. In these cases there was less eIF4E binding to the cap resin, giving further evidence that eIF4G can influence cap binding. Some antibodies also caused a decrease in eIF4E elution, indicating interference via the cap binding region.

Mapping of the antibodies gave an indication of the amino acids involved in cap/eIF4G binding. Amino acids on the surface region of eIF4E, thought to be involved in eIF4G

binding, were mutated. Mutations of hisproleu37-39, trp75, glu72, val71 and gly139 all reduced the amount of 4G-BD4E bound to eIF4E, some more than others. With these mutations the amount of eIF4E bound to the cap resin was reduced also. SPR experiments additionally showed reduced cap-binding affinities with these mutations.

These experiments repeated with p20 showed some overlap of eIF4E residues involved in binding to this protein and some that did not have such an effect on p20, indicating that the binding sites are not identical but do involve some of the same amino acids (see Figure 1.6).

1.3.2 Importance of the N-terminal region of eIF4E for binding eIF4G

Having shown that $eIF4GI_{393-490}$ binds to the N-terminal region of eIF4E, Gross *et al* (2003) looked at which residues are important for binding in the N-terminal region. They prepared truncated mutants of eIF4E deleting the first 20, 30 or 35 amino acids of eIF4E. NMR spectra of ^{15}N-labelled $eIF4GI_{393-490}$ in complex with unlabelled eIF4E mutants showed that $eIF4GI_{393-490}$ folds upon binding the Δ20 mutant, but remains mostly unfolded with the Δ30 and Δ35 mutants. This shows the first 20 amino acids are not important for binding $eIF4GI_{393-490}$.

Isothermal titration calorimetry (ITC) data showed a variation in affinities of $eIF4GI_{393-490}$ for the eIF4E mutants, with the Δ20 mutation still showing strong binding comparable with the wild type eIF4E. The Δ30 and Δ35 mutations showed a reduction in binding affinity of approximately 12-fold and 60-fold respectively. These data complement the NMR results and show the importance of the first 30-35 amino acids of eIF4E in binding $eIF4G1_{393-490}$.

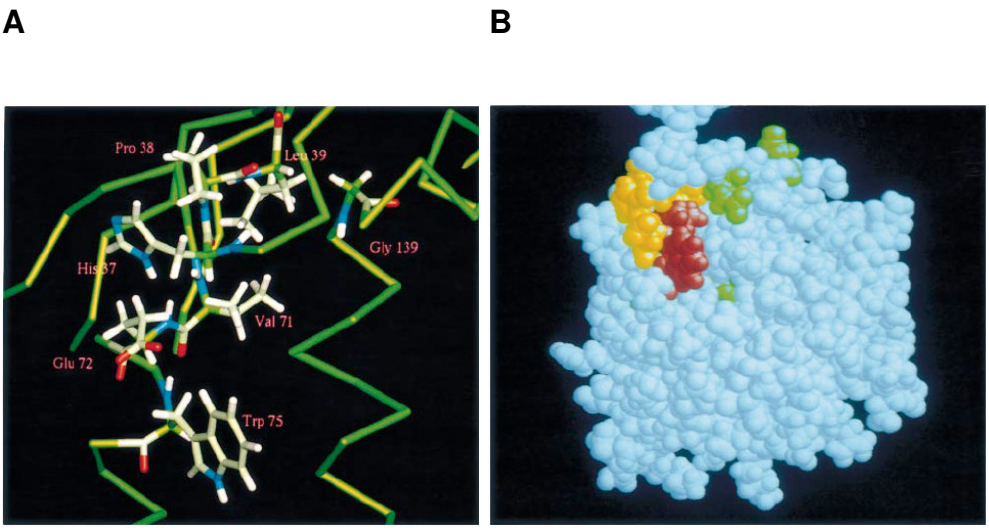

Figure 1.6 eIF4G and p20 share some of the same binding residues on eIF4E.

(A) Backbone model showing the residues involved in eIF4G and p20 binding on the dorsal surface of eIF4E. (B) Space filling model showing the same residues on the dorsal face of eIF4E. Red indicates amino acids involved in both eIF4G-BD4E and p20 binding (V71 and W75), yellow indicates those only involved in 4G-BD4E binding (E72, H37, P38, L39, G139) and green are those that have no effect on binding to either. From Ptushkina *et al* (1998).

1.4. Binding of eIF4E to 4E-BPs

1.4.1 4E-BP binding site

To determine the location of the 4E-BP binding site on eIF4E, mammalian 4E-BP2 was added to $^{1}H,^{15}N$-labelled yeast eIF4E and studied using NMR (Matsuo *et al*, 1997). The authors were looking for any changes in the chemical shift pattern caused by addition of the 4E-BP2. 4E-BP2 caused the disappearance of around 20 residues mostly centred around β-sheet b2 and b1, helix a2 and the smaller connecting loops b2 and a2, a4 and b5 and b6 and a5, indicating they were involved in binding. The biggest changes were in residues in the regions 32-50 and 62-79.

1.4.2 Human eIF4E binding to 4E-BPs

In 1999 the McCarthy group (Ptushkina *et al*, 1999) studied human eIF4E binding to human 4E-BP1 and BP2. They constructed mutations of eIF4E by changing a number of amino acids in the dorsal region, and used a yeast two-hybrid system to look at the interactions between eIF4E and its ligands.

The residues studied were hisproleu37-39, val69, glu70, trp73, gly139 and glu140 in the dorsal region of eIF4E. All except glu140 had an effect on eIF4G binding, and leu39, val69, trp73 and gly139 had an effect on 4E-BP2 binding. The notable difference between 4E-BP1 and BP2 was val69, which is involved in binding between eIF4G and 4E-BP2, but did not seem to have an effect on 4E-BP1 binding. So eIF4G and 4E-BP1 and BP2 bind to some, but not all of the same molecular contacts on eIF4E. These three ligands seem to compete for the same site but differ in respect to some of the amino acids involved in the interaction (see Figure 1.7).

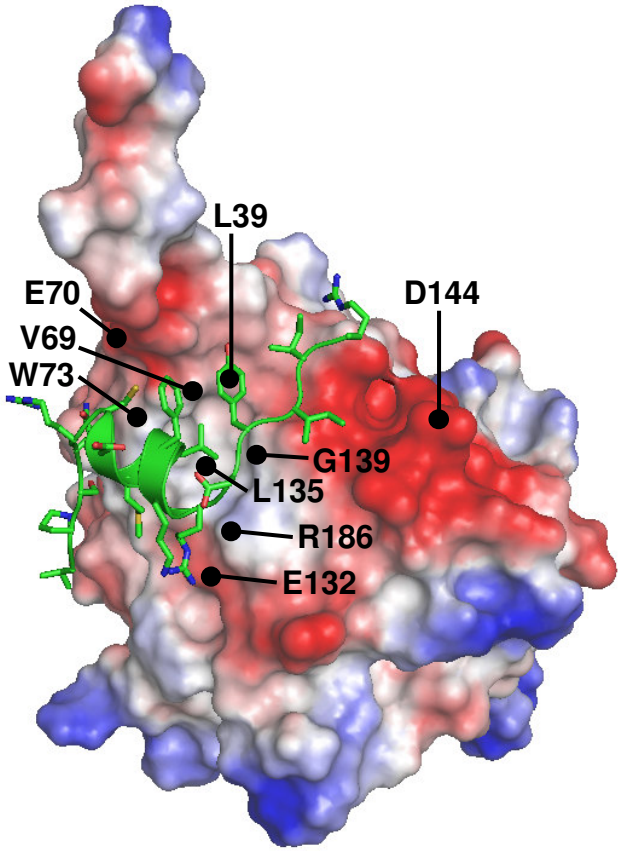

Figure 1.7 Electrostatic surface map for eIF4E.

The positions of key eIF4E residues are indicated, with 4E-BP1$_{51-67}$ superimposed (with the α-helical region highlighted). Acidic (negatively charged) regions are in red. Figure prepared by Prof Jim Warwicker. Yeast p20/eIF4G binding to yeast eIF4E, using the two-hybrid system, showed similarities to the human protein experiments, with p20 using some but not all of the amino acids involved in eIF4G binding, as previously shown (Ptushkina *et al*, 1998).

Using m^7GTP chromatography it was shown that the human 4E-BPs have the ability to increase binding of eIF4E to m^7GTP resin, indicating they can stabilise a "dead-end" complex of 4E-BP/eIF4E/m^7GTP cap.

SPR experiments were used to determine binding constants and binding interactions of the 4E-BPs to eIF4E bound to capped RNA. In the presence of the 4E-BPs, eIF4E coupled to capped RNA immobilised on a chip remained more strongly bound, having a slower "off-rate" from the chip. This showed that 4E-BPs increase the stability of eIF4E bound to capped RNA with 4E-BP1 having a lesser effect than 4E-BP2.

The binding motifs for 4E-BP1 and 4E-BP2 differ in a region of three amino acids. The MEC submotif in 4E-BP1 was mutated to LDR, which is the submotif in 4E-BP2. This mutant form of 4E-BP1 showed no interaction with the mutant val69 form of eIF4E, as with 4E-BP2, and showed an increased affinity for eIF4E. The authors devised a model for 4E-BP binding in which the binding proteins can trap eIF4E in a tightly bound complex with capped mRNA that cannot then interact with eIF4G.

The crystal structure of the human eIF4E/m^7GpppA/human 4E-BP1$_{36-70}$ peptide complex (Tomoo *et al*, 2005) also showed 4E-BP1$_{36-70}$ as having an L-shaped structure, as in previous ternary complexes. Residues in the C-terminal arg63-pro66 region of the binding motif were shown to be important, with asn64 and ser65 forming hydrogen bonds and electrostatic contacts with asn77 on eIF4E. Leu59 and arg63 form hydrogen bonds and electrostatic contacts with trp73. The arg51-phe58 region forms hydrogen bonds, electrostatic and hydrophobic interactions with the his37-gln40 N-terminal sequence of eIF4E, with tyr54 forming interactions with pro38, gly139 and val69. The arg56-cys62 helical region of the

peptide is stabilised by contacts with glu132, trp73 and his37. These residues of eIF4E were the same as those identified as important in Ptushkina *et al* (1999).

One conformational feature the authors noted was the arrangement of the asp55, lys57, glu61, arg63 residues on the solvent side of the helix formed by the binding motif. The side chains of these amino acids form an alternate acidic and basic sequence, which they suggest could be important in the function of 4E-BP1 (see Figure 1.8). This conformational feature has not been studied and could play an important part in the correct folding of 4E-BP1 which, as already discussed, is unfolded in solution and forms secondary structure on binding eIF4E. If these amino acids play a role in the structural formation of 4E-BP1 they will be important for the function of the protein as, if not folded correctly, the strength of binding will be less and 4E-BP1 will not be as efficient as a repressor of translation.

1.4.3 Importance of the N-/C-terminal region of 4E-BPs for binding eIF4E

As with eIF4G, the N-terminal 33 residues of eIF4E are important for the interaction with 4E-BP1 (Tomoo *et al*, 2006). SPR analyses were also used for comparing the peptide 4E-BP1$_{36-70}$ and the full length 4E-BP1 binding to eIF4E. The full length 4E-BP1 gave a two order of magnitude increase in association constant compared to the peptide, indicating the importance of the N-/C-terminal sequence of 4E-BP1 in binding eIF4E. This is in contrast to Marcotrigiano *et al* (1999) however, who found similar free energy values for the peptide and the full length 4E-BP1 binding to eIF4E using ITC.

The C-terminal flexible region of human 4E-BP2 may also play an important role in the interaction with eIF4E (Mizuno *et al*, 2008). N- and/or C-terminal deleted 4E-BP2 was used

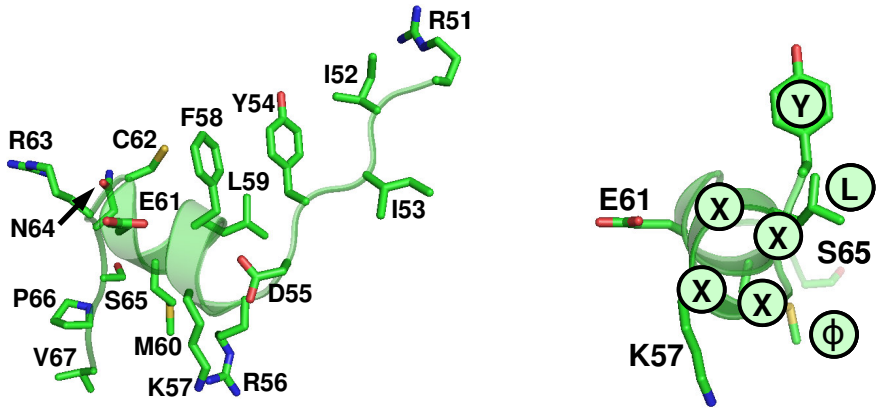

Figure 1.8 Backbone structure of 4E-BP1$_{51-67}$.

(A) A version of the backbone structure of 4E-BP1$_{51-67}$ in the conformation determined by X-ray crystallography of the eIF4E:4E-BP1 complex. Figure prepared by Prof Jim Warwicker. (B) The backbone for amino acids 54-65 of 4E-BP1 is shown, covering the helical segment, and aligned along the helix axis, as viewed from the right in panel A. S65, the Y(X)$_4$Lϕ motif and the side chains for Y54, L59, M60 (Y, L, ϕ, facing eIF4E) and for K57, E61 (solvent-facing) are highlighted.

to estimate the kinetic parameters on the interaction with m^7GTP bound eIF4E using SPR. A lack of C-terminal region changes the mode of interaction with eIF4E causing a rapid dissociation from eIF4E compared to the full length 4E-BP2, which manifests slower dissociation. A greater than 47 residue C-terminal deletion weakened the interaction with eIF4E by 3 orders of magnitude. The 32-47 residue sequence from the C-terminus of 4E-BP2 corresponds to his74-glu89 and this sequence primarily participates in the interaction with eIF4E.

The thr46-glu89 sequence of human 4E-BP2 corresponds to the 446-489 sequence of yeast eIF4G and Mizuno and colleagues (2008) used the NMR structure from Gross *et al* (2003) as a template for Molecular Dynamics simulations. Overall, the thr46-glu89 sequence of 4E-BP2 results in a right handed helical ring formation similar to that observed for the 393-490 sequence of yeast eIF4G**.** The authors propose the cys73- glu89 sequence of 4E-BP2 binds the N-terminal flexible region of eIF4E through hydrophobic interactions and the his74-glu89 sequence strengthens the binding of the $Y(X)_4L\phi$ consensus region to the eIF4E binding site.

Wang and colleagues (2003) identified two novel phosphorylation sites in the C-terminal tail of 4E-BP1 (see later). The QFEMDI motif at the C-terminus of 4E-BP1 also plays a role in phosphorylation of other sites on 4E-BP1.

1.5. Effects of phosphorylation of 4E-BPs on binding to eIF4E

1.5.1 Order of phosphorylation of 4E-BPs

The order of phosphorylation of endogenous 4E-BP1 in HEK293 cells was determined by Gingras *et al* (2003). Phosphospecific antibodies for the phosphorylation sites were developed. 2D SDS-PAGE gels were blotted to detect the different phosporylation sites. Blotting with the antibody against phosphorylated thr37/46 revealed five phosphorylated isoforms. An antibody against phosphorylated thr70 detected three isoforms, and an antibody against phosphorylated ser65 detected two isoforms. So thr37/46 is phosphorylated in the absence of other phosphorylated sites, thr70 is phosphorylated after thr37/46, then finally ser65. The fifth phosphorylation site was postulated to be ser83 or ser112.

Wang *et al* (2003) confirmed the phosphorylation site at ser112 (see below), and phosphorylation of ser101 was shown to be required for phosphorylation of ser65 as a ser65(P) antibody did not detect anything in cell extracts of cells transfected with an ser101ala mutant.

1.5.2 Phosphorylation on Ser65 causes a reduction in binding to eIF4E

Phosphorylation of eIF4E binding proteins has been shown to prevent binding to eIF4E. Initial *in vivo* studies were done using HEK293 cells transfected with plasmids expressing rat 4E-BP (PHAS-I) (Mothe-Satney *et al*, 2000). Gel mobility assays were used to determine the different phophorylated forms of PHAS-I. Cell extracts from cells transfected with PHAS-I mutated in thr36/45 or thr69 showed a reduction in the amount of phosphorylated ser64 appearing on the gel, indicating that these residues are needed for phosphorylation of ser64. Specifically, phosphorylation of ser64 on PHAS-I causes a reduction in binding to eIF4E

(Mothe-Satney *et al*, 2000). Affinity chromatography studies were used to show PHAS-I binding to FLAG-eIF4E. Binding decreased with a time course identical to phosphate incorporation on ser64 of PHAS-I. Blotting with antibodies against phosphorylated ser64 did not detect anything in fractions co-purified with eIF4E, indicating that PHAS-I phosphorylated on ser64 does not bind eIF4E.

The same is true of human 4E-BP1 (Karim *et al*, 2001). Affinity chromatography was used to look at the binding of phospholabelled human 4E-BP1 to eIF4E. Phospholabelled protein was mixed with eIF4E and the eIF4E was allowed to bind to m^7GTP resin. The proportion of bound and unbound 4E-BP1 was used to determine binding to eIF4E. 4E-BP1 phosphorylated on ser65 showed the weakest binding with 75% unbound to eIF4E compared with 80% of fully phosphorylated 4E-BP1. Then, in increasing order of binding strength, positions thr46, thr37 and ser83. The conclusion being, that phosphorylation on ser65 strongly reduces the ability of 4E-BP1 to bind eIF4E and therefore to inhibit translation.

1.5.3 Release of 4E-BPs from eIF4E

Phosphorylation of ser65 alone is not enough to cause release of 4E-BP1 from eIF4E (Gingras *et al*, 2001). Affinity chromatography of mutant thr37ala/thr46ala, ser65ala, thr70ala 4E-BP1 proteins incubated with labelled ATP and ERK2, showed that the mutant proteins were still able to bind eIF4E. Phosphorylation of the ser65 alone was not enough to prevent binding.

Phosphorylation of ser112 is also necessary for release of 4E-BP1 from eIF4E (Wang *et al*, 2003). HEK293 cells were transfected with plasmids containing mutant forms of 4E-BP1. Affinity chromatography assays and western blotting of cell extracts showed eIF4G is present

in unbound fractions on m^7GTP resin. Mutant ser112ala 4E-BP1 remains bound to eIF4E preventing binding of eIF4G to eIF4E. Ser112 did not influence phosphorylation of other sites however, so the authors propose this effect on binding must be due to direct links with eIF4E. Further, thr70 is still phosphorylated so phosphorylation of this site is not sufficient for release of 4E-BP1.

1.5.4 Biophysical studies of binding of phosphoproteins

SPR was used to measure binding affinities of asp and glu mutants of ser65 and thr46 on 4E-BP1 (Karim *et al*, 2001). The ser65glu mutation gave a 2-3-fold increase in dissociation constant compared to wild type 4E-BP1. Of the asp mutants, thr46asp and ser65asp also gave 2-3-fold increases. These results agreed with *in vivo* studies the authors did showing that ser65glu and thr46asp mutations gave a partial relief of growth inhibition.

Dissociation constants for the phosphoproteins were also determined. Phosphorylation on ser65 gave a dissociation constant two orders of magnitude greater than the unphosphorylated protein (compared with three orders of magnitude for wild type protein phosphorylated on all 5 sites). Phosphorylation on thr37/46 gave values 3-5-fold greater, and phosphorylation on ser83 gave a value less than 2-fold greater. All the above data pointed to phosphorylation of ser65 causing the greatest reduction in binding affinity, whereby mutation of ser or thr to glu or asp provided only very limited mimicry of the phosphorylation event.

Fluorescence quenching was used to determine binding constants of mono and di-phosphorylated ser65/thr70 peptides of 4E-BP1 binding to eIF4E (Gingras *et al*, 2001). The unphosphorylated 4E-$BP1_{51-67}$ peptide gave a dissociation constant of 105 nM on binding eIF4E, with the same peptide phosphorylated on ser65 having a dissociation constant of 210

nM, and the 4E-BP1$_{51-75}$ peptide phosphorylated on ser65/thr70 having a dissociation constant of 175 nM on binding eIF4E. Phosphorylation of ser65 did cause a 2-fold reduction in binding, but both peptides did bind, indicating that phosphorylation of thr37/46 is also required for release from eIF4E.

Further studies were done with a phosphoserine peptide of 4E-BP1 binding to eIF4E, using SPR (Tomoo *et al*, 2006), which also showed a two-fold reduction in binding compared to the unphosphorylated peptide. The phosphopeptide had a two-fold faster dissociation rate, although the association rates were the same for both.

1.5.5 Structural effects of Ser65 phosphorylation

How does phosphorylation of ser65 on 4E-BP1 cause a reduction in binding to eIF4E? In Figure 1.9 panel A, the ser65 side chain of the 4E-BP1 is shown close to an acidic surface feature of eIF4E. One explanation is that phosphorylation of this serine could lead to electrostatic repulsion and cause release of 4E-BP1 from eIF4E, thereby allowing translation initiation to proceed (Marcotrigiano *et al*, 1999). However, Marcotrigiano and colleagues were not able to define this relationship between 4E-BP1 and eIF4E in the region of ser65, because the electron density of their crystal structure of the ternary complex (see section 1.2.1) did not extend beyond asn64.

Another possibility is that phosphorylation of ser65 causes a change in structure of the binding site on eIF4E. Glu70 and asp71 of eIF4E are in salt bridges with the his37 and lys36 respectively (see Figure 1.9 panel B). A phosphate group on ser65 could affect the pKa value of glu70, affecting the stability of glu70-his37, so the local structure of the binding site could be affected (Karim *et al*, 2001).

Gross *et al* (2003) constructed a model to show binding of the human 4E-BP1 with human eIF4E. The mammalian 4E-BP1 from the structure in complex with murine eIF4E was superimposed on the human 4E-BP1 in the model (see Figure 1.9 panel C). Their model showed the positions of the phosphorylation sites of the 4E-BP1. Ser65 is orientated towards glu70 of human eIF4E and is in close proximity to glu61 on the peptide, which could destabilise formation of the consensus helix.

The crystal structure of the human eIF4E/m^7GpppA/human 4E-BP1$_{36\text{-}70}$ peptide complex was determined by Tomoo *et al* (2005). They gave evidence for phosphorylation of ser65 causing a shift in the structure of 4E-BP1, with the C-terminal end moving away from eIF4E and forming a more rigid conformation (see also Tomoo *et al*, 2006). This was only a simulation, however, using Molecular Dynamics calculations, and the role of phosphorylation of the 4E-BPs in terms of structural effects on the region of their 4E binding motif has remained uncharacterised.

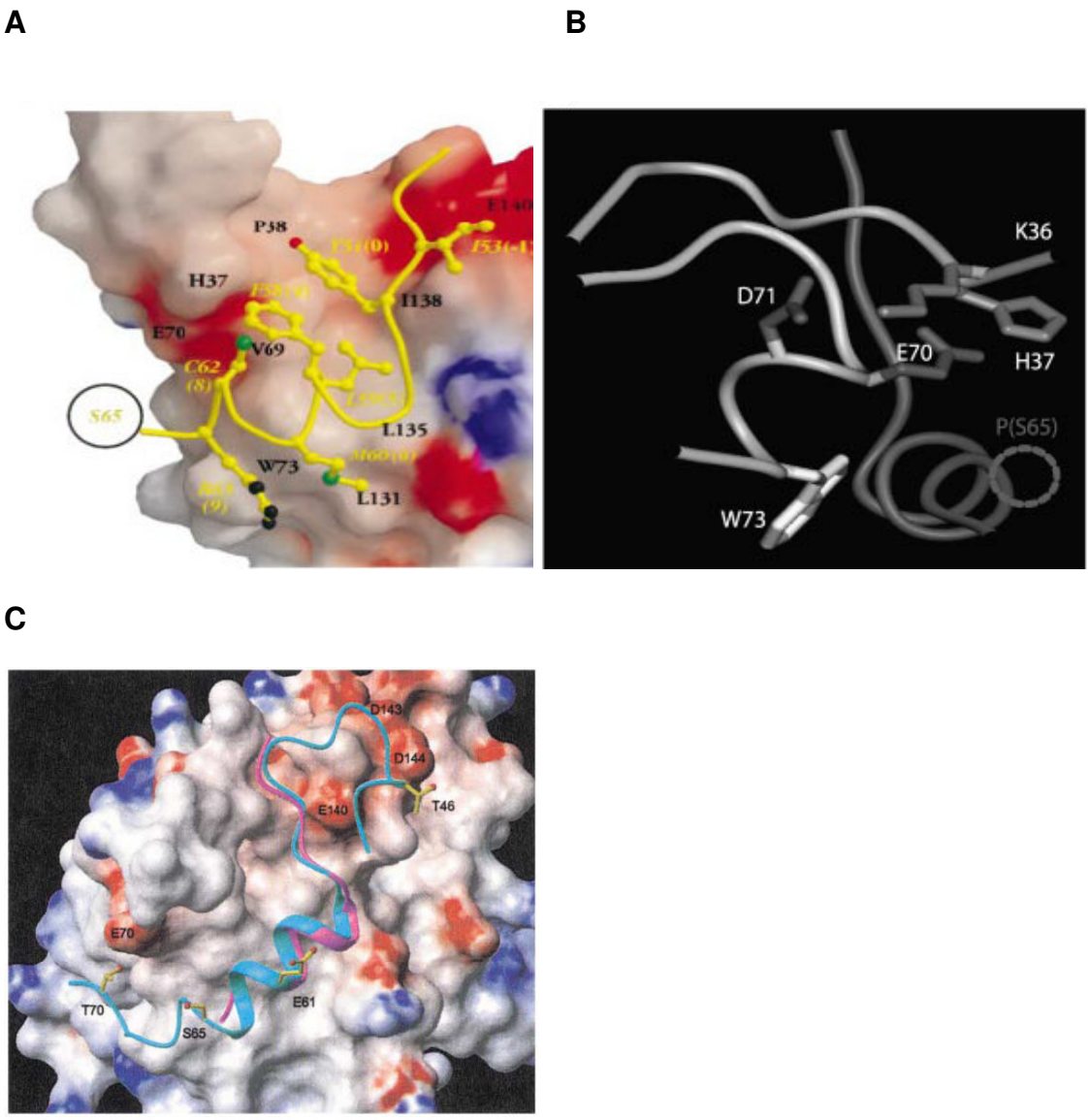

Figure 1.9 Effects of phosphorylation of Ser 65 on the interaction with eIF4E.

The S65of 4E-BP1 is close to surface features of eIF4E that cause disruption of binding on phosphorylation of S65. (A) A representation of the 4E-BP1 peptide (in yellow) overlaid on the surface of eIF4E, showing the position of the S65 side chain orientated towards the E70 of eIF4E. From Marcotrigiano *et al* (1999). (B) Backbone diagram of the interactions of eIF4E with the 4E-BP1 peptide showing the potential phosphorylation site as a dashed circle. From Karim *et al* (2001). (C) Space filling model coloured for electrostatic potential showing the human 4E-BP1 (cyan) overlaid on the mammalian 4E-BP1 (magenta). E61and three phosphorylation sites T46, S65 and T70 are shown in yellow. From Gross *et al* (2003). Phosphorylated S65 in close proximity to E61and E70 could potentially destabilise formation of the consensus helix.

1.6. Aims and Objectives

This study aims to further our understanding of the binding of human 4E-BP1 to human eIF4E, and specifically to investigate the influence of certain residues of 4E-BP1 on the interaction between 4E-BP1 and eIF4E.

It has been shown that 4E-BP1 is unstructured and folds into a helical conformation on binding eIF4E (Fletcher *et al*, 1998; Fletcher and Wagner, 1998; Marcotrigiano *et al*, 1999), but what predisposes the 4E-BP1 to fold in the correct conformation on the dorsal face of eIF4E? A number of residues of both eIF4E and 4E-BP1 which are thought to be important in the interaction between the proteins have been identified (Ptushkina *et al*, 1999; Tomoo *et al*, 2005). However the role of residues asp55, lys57, glu61 and arg63 in the binding motif of 4E-BP1 that are not directly involved in binding eIF4E is still unexplained.

Phoshorylation of 4E-BP1 causes the reduction in binding to eIF4E (Gingras *et al*, 1999). However there is still uncertainty about how this is achieved and a number of possibilities have been put forward (Marcotrigiano *et al*, 1999; Karim *et al*, 2001; Gross *et al*, 2003; Tomoo *et al*, 2005), but the role of phosphorylation of 4E-BP1 in terms of the structural effects on the region of the 4E binding motif is still unclear.

In this study a number of techniques have been employed to try and further our understanding of the role of folding in determining the affinity between eIF4E and 4E-BP1. ITC was used to determine binding affinities between peptides of 4E-BP1$_{51\text{-}67}$ and recombinant eIF4E and NMR studies were performed on ^{13}C, ^{15}N-labelled peptides in solution and titrated with recombinant eIF4E, to further investigate the role phosphorylation and residues of the eIF4E

binding motif play in binding, and may have on the secondary structure of the 4E-BP1. The NMR experiments were done in collaboration with Professor David Cowburn and Dr Kaushik Dutta at the New York Structural Biology Centre.

Materials and Methods

2.1. Strains and Plasmids

2.1.1. Escherichia coli Strains

CAG629	F⁻ *lacZ*(am) *pho*(am) *lon supC*(ts) *trp*(am) *rpsL rpoH*(am)*165* *zhg::Tn*10 *mal*(am)
Top10F'	F´{*lac*Iq Tn*10* (TetR)} *mcr*A Δ(*mrr-hsd*RMS-*mcr*BC) Φ80*lac*ZΔM15 Δ*lac*X74 *rec*A1*ara*D139 Δ(*ara-leu*)7697 *gal*U *gal*K *rps*L *end*A1 *nup*G

The CAG629 strain has a temperature sensitive supressor gene *sup*Cts and when incubated at 37 ^{o}C or 42 ^{o}C becomes deficient in expression of heat shock proteins (Grossman *et al*, 1984). This can increase the stability of foreign proteins expressed in *E. coli*. The Top10 strain was used for amplification of plasmid DNA.

2.1.2. Plasmid for expression in CAG629

The plasmid used in this study is the pCYTEXP3 plasmid (Schneppe *et al*, 1994). The pCYTEXP3 plasmid contains the strong bacteriophage λ promoters P_R and P_L under the regulation of the repressor gene *cI*ts857 (see Figure 2.1). This allows for temperature sensitive induction of expression by shifting the incubation temperature to 42 ^{o}C. The

pCYTEXP3-human eIF4E clone was previously prepared in this laboratory by Dr Md. Manjurul Karim.

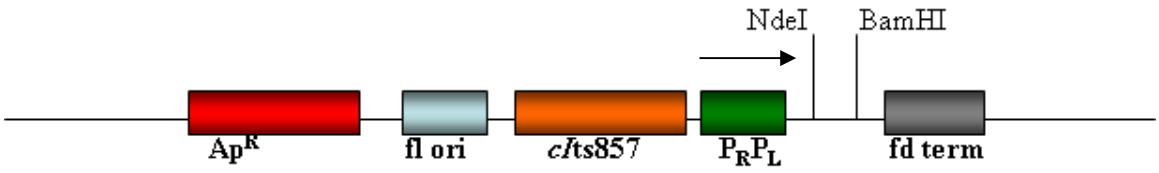

Figure 2.1 Schematic diagram of pCYTEXP3 plasmid.

Diagram illustrating major features of the plasmid including the λ promoters (green), repressor gene *cI*ts857 (orange) and antibiotic resistance gene (red). eIF4E gene was cloned between NdeI and BamHI (adapted from Schneppe *et al*, 1994).

2.2. Protein Methods

2.2.1 SDS-PAGE

Samples were run on Long-Life NuSep pre-cast Tris-HEPES protein gels, 4-20% (Generon), with a Tris-HEPES-SDS running buffer, in a BIORAD Mini-PROTEAN system. Samples were visualised under UV illumination using a Kodak Gel Logic system.

2.2.2 Measurement of protein concentration

45 µl bovine serum albumin (BSA) 1 mg/ml was diluted with 135 µl water to give 180 µl BSA 250 µg/ml. Then the following dilutions were prepared in water:

	250µg/ml BSA (µl)	Water (µl)	[BSA] µg/ml
Blank	-	50	0
1	2	48	10
2	5	45	25
3	10	40	50
4	20	30	100
5	30	20	150
6	40	10	200
7	50	-	250

Samples to be measured were diluted in water to 50 µl volume. One volume bicinchoninic acid (BCA) reagent (Sigma) was mixed with one fiftieth volume copper sulphate solution (Sigma), sufficient for the total number of samples and standards. 450 µl of this mixture was added to each 50 µl sample/standard and incubated for between 30 min and one hour at 37 ^{o}C. Absorbance was measured at 562 nm.

2.2.3 Expression of recombinant eIF4E

E. Coli CAG629 cells transformed with pCYTEXP3-human eIF4E plasmid were inoculated in 2 ml LB Broth Miller (Formedium) and grown at 30 ^{o}C overnight. Overnight culture was used to inoculate 200 ml culture, which was again grown overnight. These 200 ml were then used to inoculate 4 l of culture which was grown to an OD of 0.4-0.6. Cells were then induced by rapid heating to 42 ^{o}C and induction continued at 42 ^{o}C for 4 hours. Cells were induced by heat induction as this strain of cells is deficient in proteases at higher temperatures, which helps to protect foreign proteins. The protein forms in inclusion bodies which also has the advantage of protecting against degradation. Optimal expression time was

previously determined by Dr Md. Manjurul Karim to be 4 hours. Cells were harvested by centrifuging for 10 min at 6000 rpm, using a Beckman Avanti J-25 centrifuge, and then washed once with water and centrifuged for 10 min at 8000 rpm using a Beckman Avanti 30 centrifuge. Cell pellets were stored at -20 ^{o}C.

2.2.4 Purification of recombinant eIF4E

2.2.4.1 Lysis from inclusion bodies

Buffer A	Buffer B
20 mM HEPES/KOH pH7.4	20 mM HEPES/KOH pH7.4
0.1 M KCl	1 M KCl
0.2 mM EDTA	0.2 mM EDTA

Lysis Buffer	Wash Buffer	Denaturing Buffer
20 mM HEPES/KOH pH7.4	20 mM HEPES/KOH pH7.4	6 M guanidine hydrochloride
0.5 M KCl	0.2 mM EDTA	0.25 M DTT in buffer A
0.2 mM EDTA	2% Triton X-100	
2% Triton X-100		

Cells were resuspended in lysis buffer plus 1% phenylmethanesulphonylflouride (PMSF) and one tablet of protease inhibitor cocktail tablets (EDTA free, Roche). Suspension was sonicated by 6 x 30 s pulses at 90% power with 30 s intervals using a Bandelin Sonopuls sonicator. Sonicate was clarified by centrifuging for 30 min at 9800 rpm using a Beckman Avanti 30 centrifuge. Inclusion bodies were washed twice with wash buffer, then resuspended in denaturing buffer and placed in a shaking incubator at 50 ^{o}C for 2-3 hours, until pellet resuspended. Suspension was allowed to cool to room temperature, mixed with an equal volume of buffer A, then dialysed into 5 l of buffer A overnight. Buffer was changed the next morning (a white precipitate forms) and again in the evening and dialysis continued overnight. The lysate was clarified by centrifuging for 20 min at 20,000 g.

2.2.4.2 Purification on m^{7}-GTP sepharose resin

Supernatant was then incubated with 1 ml bed volume of m^{7}-GTP sepharose 4B resin (GE Healthcare), equilibrated with buffer A, on a roller for 2 hours at 4 ^{o}C. Slurry was poured into a disposable column (BioRad) and allowed to drain by gravity. Resin was washed with 3 x 10 ml buffer A and then 10 ml buffer A plus 0.1 mM GDP. eIF4E was then eluted with 6 x 1 ml buffer A plus 0.1 mM m^{7}-GTP. Eluted fractions were then dialysed into 5 l buffer B overnight. Buffer was then exchanged for 5 l buffer A and dialysis continued for at least 6 hours. Purified eIF4E protein was stored at -80 ^{o}C.

2.2.5 Preparation of eIF4E for NMR studies

eIF4E expressed from 40 l of culture was purified as described above. A final dialysis step was added with the eIF4E being dialysed into the buffer for NMR (10 mM Tris, pH 6.5, 50

mM KCl). Protein was concentrated in four aliquots of ~30 μM each and lyophilised overnight before being sent to the New York Structural Biology Centre. There the protein was resuspended in an equal volume of water and concentrated further to ~85 μM for use in NMR studies. Sample was clarified by centrifuging at maximum speed in a benchtop centrifuge.

2.3. Synthesis of Peptides

Peptides were synthesised on an Advanced Chemtech APEX 396 synthesiser, using F-moc protected amino acids purchased from Novagen/GATC Biotech. Two peptides were synthesised with the sequences RIIYDRKFLMECQNSPV and RIIYDRKFLEECRNSPV. The peptides were cleaved from the resin using 94.5% TFA, 2.5% water, 2.5% EDT, 1% TIS. The resin was washed twice with TFA to elute off the peptide and the volume reduced to around 5-7 ml. The eluate was then added to 20 ml ether to precipitate the peptide overnight at -20 ^{o}C. Peptide was pelleted by centrifugation at 20,000 g for 20 min, the supernatant removed, followed by a second wash with ether and precipitation. The pellet was dried, resuspended in water, lyophilised and stored at -80 ^{o}C.

Lyophilised peptide was resuspended in 500 μl water + 0.1% TFA and purified by HPLC on an Agilent 1100 series system, using a Luna 5micron C18 column (250 x 100 mm) by Phenomenex. The gradient used was as follows:

Time (min)	% B (acetonitrile + 0.1% TFA)
4	20
30	48
31	95
37	95
38	5
48	5
49	5

The met60glu peptide eluted off the column at 33.8-34.3% acetonitrile. The arg63gln peptide eluted at 35.4-36.1% acetonitrile. Peaks at these times were collected and lyophilised. A small amount of the lyophilised peptide was put over the column again to check purity, and subjected to MALDI-TOF mass spectrometry to confirm the correct molecular weight. Calculated molecular weight of the met60glu peptide was 2138.7 (mass spectrometry confirmed 2139.79-2140.71). Calculated molecular weight of the arg63gln peptide was 2112.7 (mass spectrometry confirmed 2112.17). All other peptides were purchased from Peptide Protein Research Ltd. Sequences for all peptides used in this study are listed in Table 2.1.

2.4. DNA Methods

2.4.1 Transformation of E. Coli cells

Cells were thawed on ice, gently mixed with 2 µl of miniprep DNA, and further incubated on ice for 20 min. Cells were then heat shocked at 37 ^{o}C for 5 min, then transfered back to ice

MUTATION	PEPTIDE SEQUENCE
Wild Type	RIIYDRKFLMECRNSPV
D55E	RIIYERKFLMECRNSPV
D55S	RIIYSRKFLMECRNSPV
K57E	RIIYDREFLMECRNSPV
K57R	RIIYDRRFLMECRNSPV
K57E/E61G	RIIYDREFLMGCRNSPV
K57E/E61K	RIIYDREFLMKCRNSPV
M60A	RIIYDRKFLAECRNSPV
M60E	RIIYDRKFLEECRNSPV
M60T	RIIYDRKFLTECRNSPV
E61A	RIIYDRKFLMACRNSPV
E61K	RIIYDRKFLMKCRNSPV
R63Q	RIIYDRKFLMECQNSPV
N64S	RIIYDRKFLMECRSSPV
S65+P	RIIYDRKFLMECRNS*PV

S*=Phosphoserine

Table 2.1 Sequences of peptides used in this study.

for 2 min. One ml of LB media was added and then cells incubated with shaking at 30 ^{o}C for 30 min-1 hour. Cells were pelleted for 2 min at maximum speed in a benchtop centrifuge and ~800 µl of the media removed. Cell pellet was resuspended in the remainder of the media and plated onto LB agar plates with ampicillin 100 µg/ml. Plate was incubated at 30 ^{o}C overnight.

2.5. Isothermal Titration Calorimetry

2.5.1 The Calorimeter

There are two cells in the instrument: one is a reference cell and one is the sample cell which contains the protein of interest (in this case eIF4E). A constant power is applied to the reference cell to maintain the temperature that is set, and this directs a feedback circuit to heat or cool down the sample cell to maintain the same temperature as the reference cell. The ligand (in this case the peptide) is injected, in known volumes, into the sample cell and this causes a heat of reaction. In an exothermic reaction the temperature will increase and this causes the feedback power to be decreased, so the temperature will return to the same as the reference cell. In an endothermic reaction the feedback power will be increased to increase the temperature in the sample cell. Measurements are plotted as the power needed to maintain equal temperature between the cells over time.

2.5.2 Preparation of samples

2.5.2.1 Preparation of eIF4E

eIF4E was dialysed twice into filtered and degassed sample buffer (10 mM Tris, pH 6.5, 50 mM KCl). Protein was concentrated using Sartorius Vivaspin 6 ml concentrators with 10,000 Da MWCO. Samples were clarified by centrifuging at full speed for 1 min in benchtop

centrifuge. Measurement of concentration was by BCA assay using reagents from Sigma (see section 2.2.2).

2.5.2.2 Preparation of peptides

The second dialysis buffer was also used to resuspend each peptide. Peptide was weighed out (~0.8 mg) and resuspended in 1 ml of buffer. After diluting to desired concentration (see below), the peptide pH was adjusted to the same pH as eIF4E using 0.2 M KOH. pH was within 0.1 units. Peptide concentration was confirmed by BCA assay. Due to aggregation of the lys57glu and lys57glu/glu61gly peptides, they were resuspended in ~1-2% dimethylsulphoxide (DMSO).

2.5.3 Isothermal titration calorimetry conditions

Isothermal titration calorimetry was performed on a VP-ITC machine (MicroCal). ~10 μM of purified eIF4E was used in the cell, and ~100-300 μM of peptide in the syringe.

ITC parameters:

No of injections	20
Volume of Injections	15 μl
Cell Temperature	25 ^{o}C
Reference Power	16 (μCal/s)

Delay (sec)	60
Stirring Speed	310

2.6. Circular Dichroism

Circular dichroism was performed on a Jasco J-810 machine. Peptides were resuspended in the same buffer used for ITC (see above) at a concentration of 14.5 μM. Samples were placed in a 1 cm cuvette. For experiments with trifluoroethanol (TFE), peptides were resuspended in the same buffer with either, 5, 10, 25 or 40% TFE.

CD parameters:

SCAN RANGE	190-250 nm
SENSITIVITY	100 mdeg
BAND WIDTH	1 nm
SCAN SPEED	50 nm/min
RESPONSE	1 s
DATA PITCH	0.2 nm
ACCUMULATE	100

2.7 Nuclear Magnetic Resonance

The NMR experiments in this study were done in collaboration with the New York Structural Biology Centre. Dr Kaushik Dutta performed all the following NMR experiments and analyses on the peptides and complexes. Experiments were performed at 25 ^{o}C using 500- and 700-MHz Bruker spectrometers.

Chapter Three

Results and Discussion

3.1 Purification of recombinant eIF4E

eIF4E is the cap binding protein and this was used to advantage in the purification by binding to an m^7GTP sepharose resin as described in materials and methods. Using this method, eIF4E was successfully purified to a high level of purity as shown in Figure 3.1. eIF4E purified in this way was used for each of the following biophysical experiments used in this study.

3.2 Influence of residues of the eIF4E binding motif of 4E-BP1 on binding to eIF4E

We wanted to investigate the role of a number of residues in the correct folding and binding of 4E-BP1 to eIF4E, in particular residues on the solvent face of the 4E-BP1 when bound to eIF4E. The residues chosen for investigation in this study were asp55, lys57, met60, glu61, arg63 and asn64. Peptides were synthesised with the sequence of human 4E-BP1, residues 51-67, with mutations of these residues, as described in materials and methods. The peptides were used, along with recombinant human eIF4E, in ITC studies to determine the effects of the various mutations on binding (summarised in Table 3.1 and Figure 3.2). ITC was used as it is potentially superior to surface plasmon resonance, which involves binding tagged protein

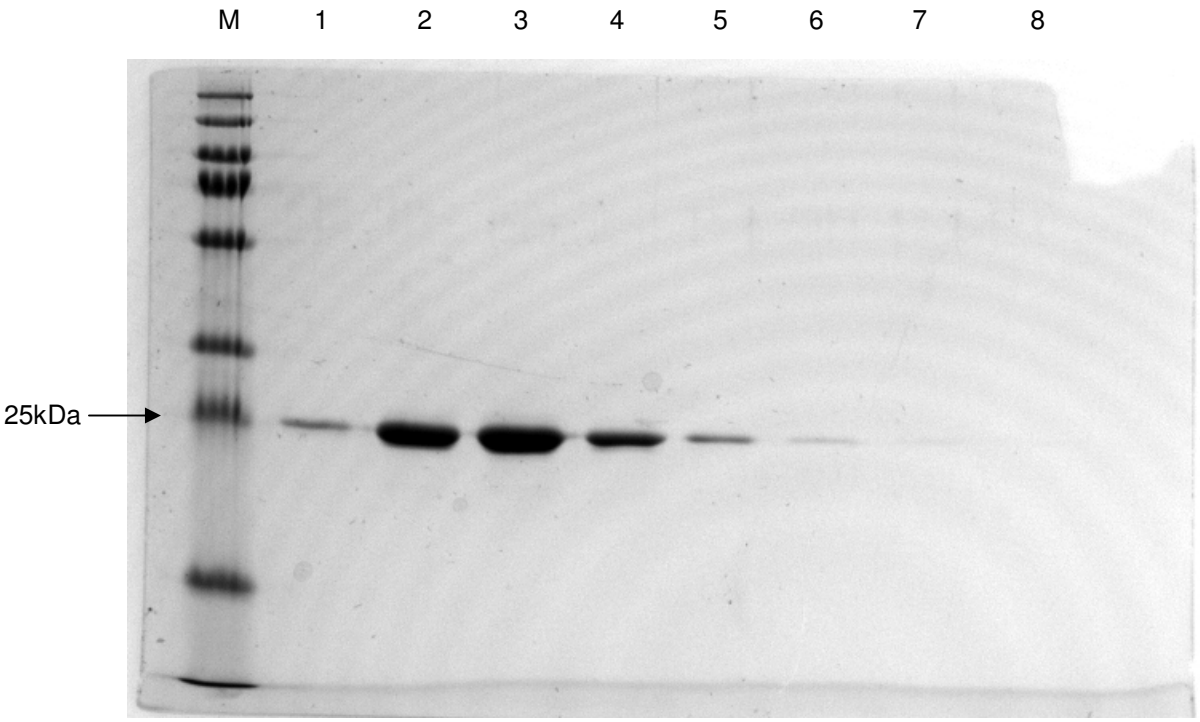

Figure 3.1 Elutions of eIF4E from m^7GTP sepharose resin.

Elutions were performed in 8 x 1 ml fractions with 0.1 mM m^7GTP in buffer A (as materials and methods). 9 µl of each fraction were ran on a Long-Life NuSep precast Tris-HEPES protein gel 4-20% (Generon). M (marker), lanes 1-8 (elutions 1-8).

to a chip and washing the ligand over the chip. ITC is regarded as a more accurate method as the protein and ligand are in solution, free to bind, without the protein of interest being tagged or bound to a chip.

3.2.1 ITC data for peptide-eIF4E pairs and role of salt bridges in stabilising α-helical conformation

The residue on the 4E-BP1$_{51-67}$ peptide that seemed to have the strongest effect on binding to eIF4E was the lys residue at position 57. Lys has a long flexible side chain with a positively charged end and is found on hydrophilic surfaces. When changed to glu this did give a strong reduction in binding (26-fold). There are a number of intramolecular salt bridges which have been identified within the eIF4E binding domain (Tomoo *et al*, 2005, supplemental data). Changing the residue at position 57 to a glu could disrupt a salt bridge with the glu at position 61, preventing the helix forming the correct conformation. As a control, changing lys57 to arg caused no change to binding affinity, so the reduction in binding seen with the lys57glu mutation can be said to be due to the change in charge at this position.

The next mutation of the 4E-BP1$_{51-67}$ peptide was changing the met at position 60 to a glu, a thr and an ala. These gave reductions in binding of the peptide to eIF4E of 11-fold, 11-fold and 23-fold respectively. Met interacts with trp73 on the surface of eIF4E and tyr54 within the binding motif, both of which have aromatic rings. The methyl group on met was changed to either an acidic, negatively charged group (glu), a hydroxyl group (thr) or a small neutral amino acid (ala), so this could interfere with the van der Waals interactions with the aromatic ring. These mutations could also disrupt a number of intramolecular salt bridges within the peptide, one of which has been shown to be with lys57.

^{51}RIIYDRKFLMECRNSPV^{67}	K_D (eIF4E)	Factor increase in K_D
Wild type	2.1x10-8 M	
D55E	2.9x10-8 M	1.4
D55S	1.0x10-7 M	4.8
K57E	5.5x10-7 M	26
K57R	1.8x10-7 M	0.86
K57E/E61G	5.2x10-7 M	25
K57E/E61K	2.1x10-8 M	1.0
M60E	2.3x10-7 M	11
M60T	2.3x10-7 M	11
M60A	4.8x10-7 M	23
E61K	3.0x10-8 M	1.4
E61A	5.2x10-8 M	2.5
R63Q	6.7x10-8 M	3.2
N64S	6.7x10-8 M	3.2
S65+P (pH 6.6)	1.2x10-7 M	5.7
S65+P (pH 6.9)	1.6x10-7 M	7.6
S65+P (pH 7.4)	2.4x10-7 M	11

Table 3.1 Dissociation constants for peptides binding to eIF4E.

Table of peptides used in this study and dissociation constants on binding to eIF4E as determined by ITC. Final column is the factor increase in dissociation constant for each mutant peptide compared to the wild type sequence. Values are averages of data calculated from at least two ITC titrations.

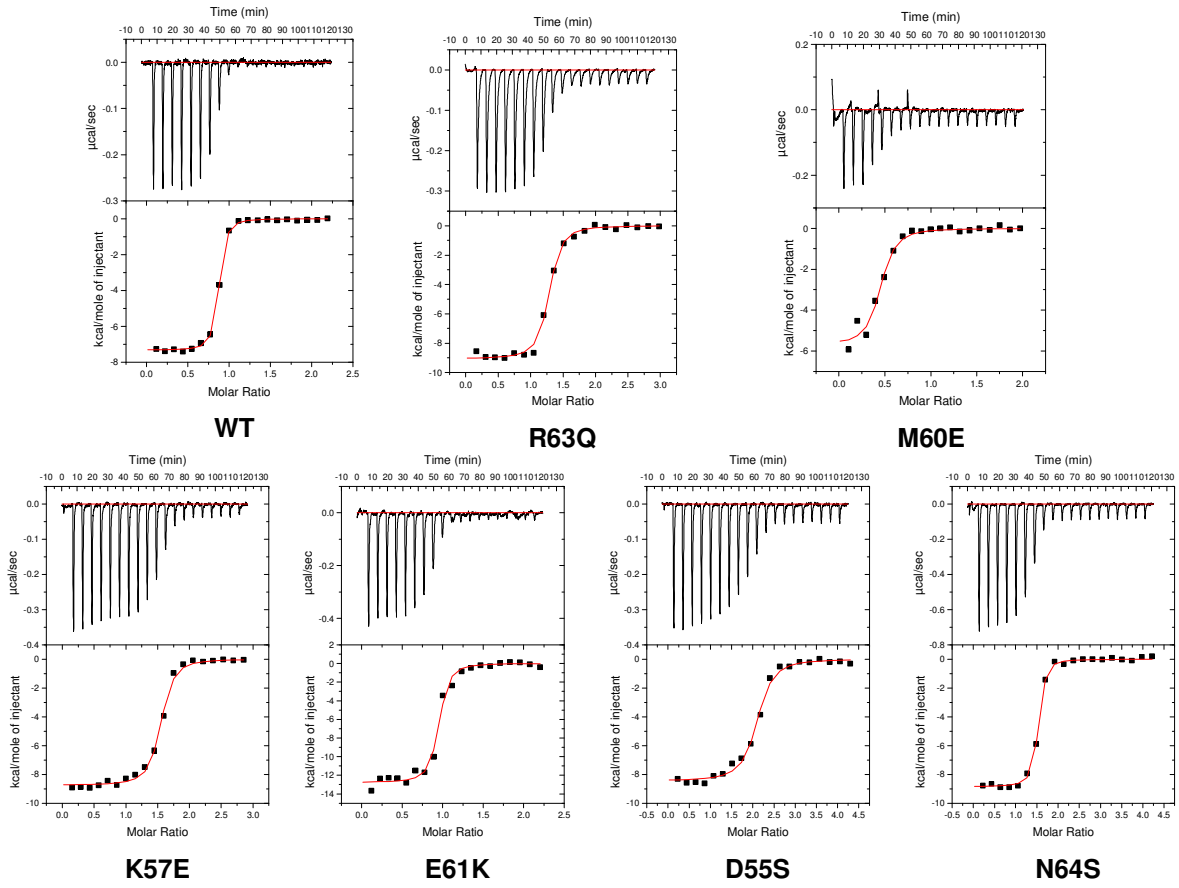

Figure 3.2 ITC plots for 4E-BP1$_{51-67}$ peptides binding to eIF4E.

Representative plots of ITC titrations for named 4E-BP1$_{51-67}$ peptides binding to eIF4E.

The asp55glu mutation changed one acidic residue for another and there was effectively no change in affinity between the 4E-BP1$_{51-67}$ peptide and eIF4E. The asp55ser mutation changed the carboxyl group to a hydroxyl and this gave a 5-fold reduction in binding between the peptide and eIF4E, which could be due to disruption of intramolecular salt bridges with lys57.

The glu61 of the 4E-BP1$_{51-67}$ peptide was changed to ala and this gave a 2.5-fold reduction in binding between the peptide and eIF4E. Changing this glu to lys seemed to give no significant change in affinity between the peptide and eIF4E. In this case it is possible the lys could still act as a donor to form intramolecular hydrogen bonds within the peptide and so conformation is maintained.

The arg63gln mutation of the 4E-BP1$_{51-67}$ peptide gave a 3-fold reduction in binding of the peptide to eIF4E. Gln has a carboxyl group in place of the amine group in arg, so this reduction in binding could be due to disruption of intramolecular salt bridges between arg63 and met60. Arg63 also forms van der Waals contacts with trp73 on the surface of eIF4E and this mutation could also disrupt this contact.

The next mutation of the 4E-BP1$_{51-67}$ peptide was asn64ser. This gave a 3-fold reduction in binding of the peptide to eIF4E. Asn is similar to asp but has an amide group instead of a carboxyl group and was changed to ser which has a short hydroxyl group. Asn64 forms salt bridges directly with asn77 on eIF4E.

The lys57glu/glu61gly double mutation of the 4E-BP1$_{51-67}$ peptide gave a 25-fold reduction in binding to eIF4E. This could have the effect of disrupting a number of intramolecular salt bridges, in particular between lys57 and glu61. With the lys57glu/glu61lys mutation, the dissociation constant was the same as with the wild type peptide. It could be that keeping this pairing of residues together allows the binding to remain the same. The salt bridge that forms

between the lys57 and glu61, within the 4E-BP1 eIF4E binding domain, may still form if there is still a lys and glu at those positions, even in the opposite orientation. Changing the glu to gly could possibly disrupt this salt bridge and give rise to the 25-fold reduction in binding that is seen.

The ITC results show that these solvent facing residues, although not all directly involved in binding, may play a role in the correct folding of the peptide into a conformation favourable for binding.

3.2.2 NMR indicates conformational changes between wild type and mutant peptides

To investigate whether these mutations do cause a change in the structure of the peptide, ^{13}C-^{15}N labelled peptides of the wild type, met60glu and arg63gln 4E-$BP1_{51-67}$ were used in the NMR studies. The peptides were also titrated with non-labelled recombinant eIF4E for structural studies of the complex.

Comparing the ^{1}H-^{15}N heteronuclear single quantum correlation (HSQC) spectra of the wild type peptide with the met60glu and arg63gln peptides shows chemical shift changes in peaks between the spectra indicating structural changes beween the wild type and mutant peptides (see Figure 3.3). In the spectra for the met60glu peptide there are chemical shift changes in the peaks corresponding to arg56, leu59, arg63 and asn64. Changing met to glu at position 60 is causing structural changes in the region of these residues, which are part of the α-helical eIF4E binding region.

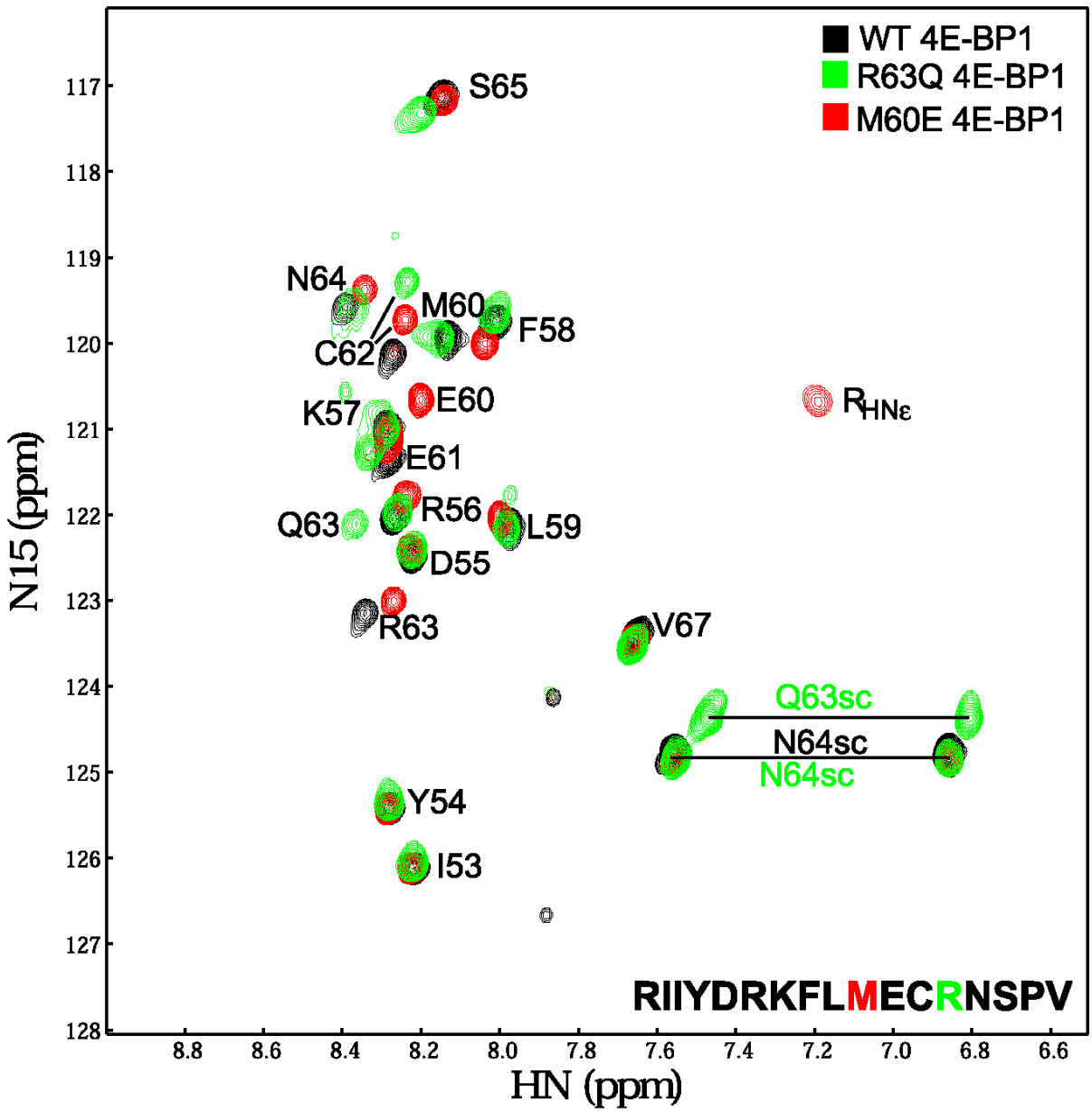

Figure 3.3 NMR spectra of 4E-BP1$_{51-67}$ peptides.

Overlaid ^{1}H-^{15}N HSQC spectra of wild type peptide (black peaks), R63Q peptide (green peaks) and M60E peptide (red peaks) with assignments. The $R_{HN\varepsilon}$ peak is the R epsilon proton. Image prepared by Dr Kaushik Dutta.

The same is true of the arg63gln peptide. Comparison with the wild type spectra shows the chemical shift changes of peaks corresponding to lys57, glu61 and to a lesser extent met60 and val67 (see Figure 3.3). The peaks corresponding to phe58 and cys62 changed position in both the met60glu and arg63gln peptides. The N-terminal residues of the peptide were largely unaffected. These results confirm the ITC data that the solvent facing residues may be important for the correct folding of the 4E-BP1 on binding eIF4E.

3.3 Effect of phosphorylation of 4E-BP1on Ser65 on binding to eIF4E

3.3.1 ITC data for phosphopeptide-eIF4E pairs and effect of charge on stabilising a-helical conformation

We next wanted to investigate further the role of phosphorylation in the folding of the peptide and the influence of charge at the C-terminal end of the eIF4E binding motif. A peptide was synthesised with the sequence of 4E-BP1$_{51-67}$ phosphorylated on the ser65 residue, and titrated with recombinant eIF4E in ITC studies.

To investigate whether the effect of phosphorylation on ser65 is pH dependent, in pH was adjusted to different levels in the ITC experiments to determine the effect on binding (results summarised in Table 3.1 and Figure 3.4). At pH 6.6 the factor increase in dissociation constant was 5.7, at pH 6.9 the factor increase in dissociation constant was 7.6, and at pH 7.4 the factor increase in dissociation constant was 11. The binding of the peptide to eIF4E decreased as the pH increased. These results further indicate the importance of charge on the phosphorylated 4E-BP1$_{51-67}$ peptide on its binding to the eIF4E.

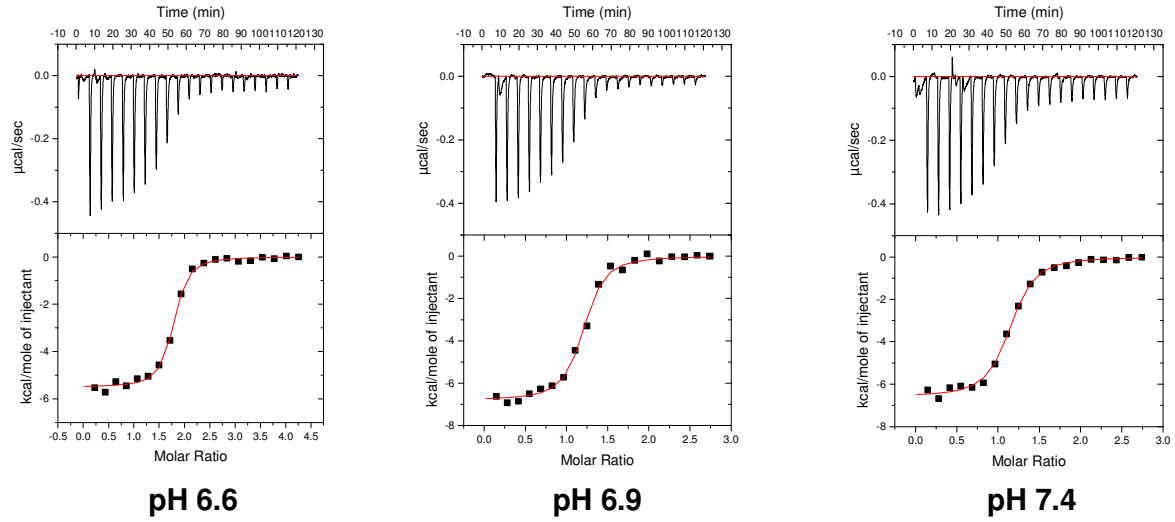

Figure 3.4 ITC plots for phosphopeptide binding to eIF4E.

Representative plots of ITC titrations for the 4E-BP1$_{51-67}$ peptide phosphorylated on S65 binding to eIF4E. Experiments were performed at three different pH values.

3.3.2 NMR indicates conformational changes between wild type and phosphopeptide and differences between the complexes with eIF4E

We then investigated whether this phosphorylation causes changes in the structure of the peptide. The ^{1}H-^{15}N HSQC spectra of the wild type 4E-BP1$_{51-67}$ peptide in comparison to the phosphopeptide shows chemical shift changes for the residues arg63, asn64 and val67 (see Figure 3.5). The phosphorylation at ser65 appears to be having an effect on the residues surrounding it at the C-terminal end of the eIF4E binding motif. The spectra of the wild type 4E-BP1$_{51-67}$ peptide and the phosphopeptide in complex with eIF4E show a number of chemical shift changes between the two, with peaks circled in blue showing differences, and peaks circled in red showing those residues which have remained the same. The spectra are consistent with the idea that the phosphopeptide does confer a number of structural changes within the complex and has an effect on the C-terminal end of the eIF4E binding region causing a change in the folding of the 4E-BP1$_{51-67}$ peptide, perhaps preventing binding to eIF4E.

3.4 CD data confirm structural differences between peptides

To confirm structural differences between the peptides CD studies were perfomed. Although the peptides are largely unstructured, when subjected to CD spectroscopy small differences in the structure of the peptides can be seen. Of particular note is the effect of the lys57glu mutation on the structure of the peptide. The CD spectroscopy showed that this peptide has the largest change in structure of all the peptides compared to the wild type (see Figure 3.6), with a more pronounced shoulder at 210-220 nm indicating a higher degree of β-sheet. This confirms results from the ITC data that this mutation has a strong effect on the structure of

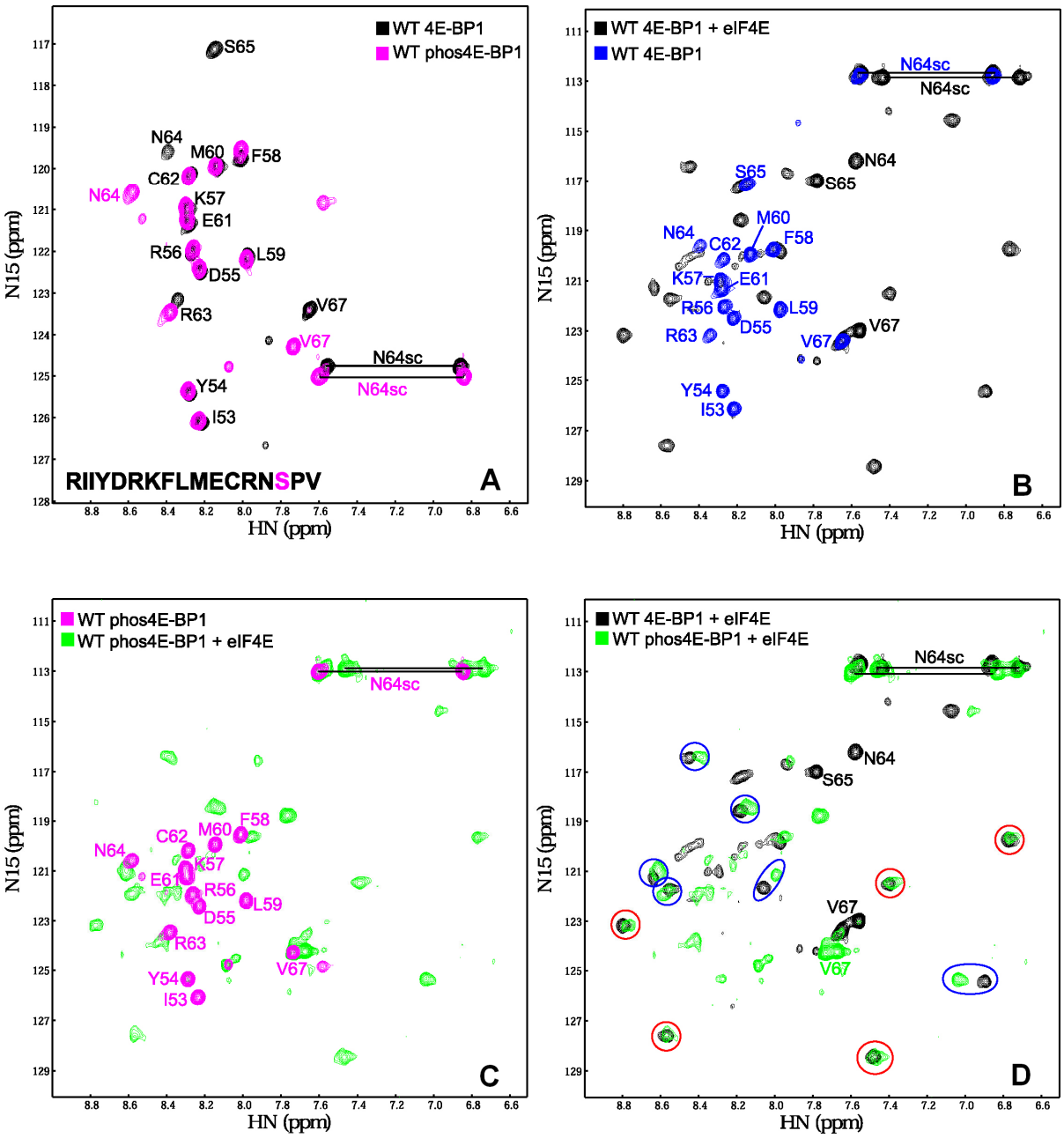

Figure 3.5 NMR spectra of 4E-BP1$_{51-67}$ peptides titrated with eIF4E.

^{1}H-^{15}N HSQC spectra of (A) wild type peptide (black) overlaid with phosphopeptide (pink). (B) Wild type peptide (blue) overlaid with wild type peptide in complex with eIF4E (black). (C) Phosphopeptide (pink) overlaid with phosphopeptide in complex with eIF4E (green). (D) Wild type peptide in complex with eIF4E (black) overlaid with phosphopeptide in complex with eIF4E (green). Images prepared by Dr Kaushik Dutta.

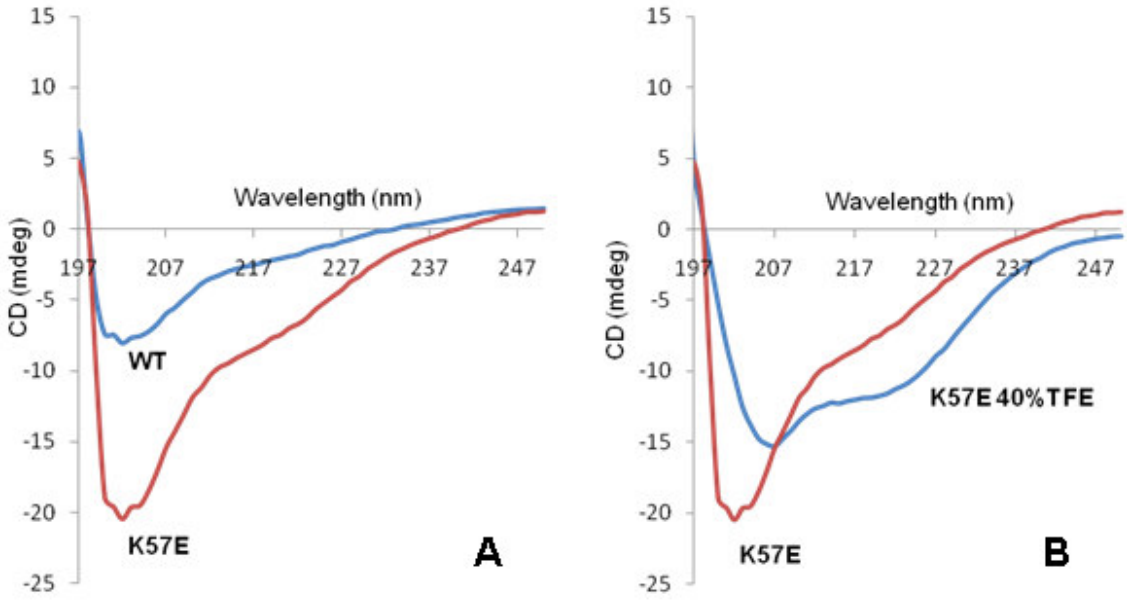

Figure 3.6 CD spectra of wildtype peptide and K57E peptide.

(A) CD spectra of the K57E peptide (red) superimposed on the wild type peptide (blue). (B) CD spectra of the K57E peptide (red) superimposed on the K57E peptide resuspended in 40% TFE (trifluoroethanol; blue).

the peptide, although causing the peptide to aggregate, which meant that DMSO had to be used in the ITC experiments. A known promoter of α–helical formation triflouroethanol (TFE; Rohl *et al*, 1996), was used to reverse this partial conversion to β–sheet (see Figure 3.6 for spectra with 40% TFE). Taken together these results suggest the lys57 residue in the eIF4E binding domain of 4E-BP1 plays an important role in the integrity of the α-helical structure of the eIF4E binding domain, which in turn does indeed influence the strength of binding of 4E-BP1 to eIF4E.

Chapter Four

Conclusions and Future Perspectives

This study has investigated the role of a number of residues in the correct folding and binding of 4E-BP1 to eIF4E, in particular residues on the solvent face of the 4E-BP1 when bound to eIF4E, using ITC, NMR and CD techniques. The dissociation constants for binding of peptides of 4E-BP1$_{51-67}$ to recombinant eIF4E, calculated by ITC, show the importance of these residues in the correct binding of 4E-BP1 to eIF4E. Although not all are involved in direct interaction with eIF4E, the ITC data showed that mutating the residues asp55, lys57, met60, glu61, arg63 and asn64 gives the 4E-BP1$_{51-67}$ peptide a reduced affinity for binding to recombinant eIF4E. The mutations could have caused the disruption of a number of intramolecular salt bridges within the peptide indicating the importance of the correct folding of 4E-BP1 on binding eIF4E. In particular lys57 and glu61 were found to be important for maintaining the integrity of the eIF4E binding region.

These ITC results are also consistent with data indicating the role of residues met60 and arg63 of 4E-BP1 in direct binding to eIF4E (Tomoo *et al*, 2005). Further, the NMR data shows the importance of these residues in intramolecular contacts within the eIF4E binding region and how they may influence the structure of the 4E-BP1 on binding eIF4E. Both the met60 and arg63 mutations affected numerous residues throughout the binding motif including phe58, cys62 and val67 on the C-terminal end of the binding motif.

One of the other questions we asked was how phosphorylation of ser65 within the eIF4E binding motif affects binding of the 4E-BPs to eIF4E. One of the factors that could account for the reduction in binding of the phosphorylated 4E-BP1 to eIF4E is charge repulsion between the phosphate group and the glu70 residue on eIF4E (Marcotrigiano *et al*, 1999). We have shown charge does have an effect on the binding of the phosphopeptide 4E-BP1$_{51-67}$ to eIF4E. The values of the dissociation constants for the unphosphorylated peptide and phosphopeptide are in the same range as those of Gingras *et al* (2001) and Tomoo *et al* (2006). However our NMR experiments have shown that there are chemical shift changes in the structure of the phosphopeptide in solution and when the phosphopeptide is in complex with eIF4E. Phosphorylation seems to have an effect on residues arg63, asn64 and val67 surrounding the ser65 at the C-terminal end of the eIF4E binding motif causing a change in the folding of the peptide on binding eIF4E. So our model of the binding of 4E-BP1 to eIF4E indicates that the effect of phosphorylation on ser65 on binding affinity is due to a reduced propensity to fold into the correct conformation for binding. This causes the disorder-order transition to favour the unfolded form that cannot bind eIF4E (see Figure 4.1).

This is consistent with the model of Gross *et al* (2003) in which phosphorylation of ser65 could destabilise formation of the consensus helix. In this model ser65 is orientated towards glu70 of human eIF4E and is in close proximity to glu61 on the peptide. In the study by Ptushkina *et al* (1999) a mutation of eIF4E of glu70ala did not influence binding to wild type 4E-BP1 in a yeast two hybrid experiment, but further studies with mutations of eIF4E at the glu70 residue in ITC experiments could further elucidate the role this residue has on binding the phosphopeptide.

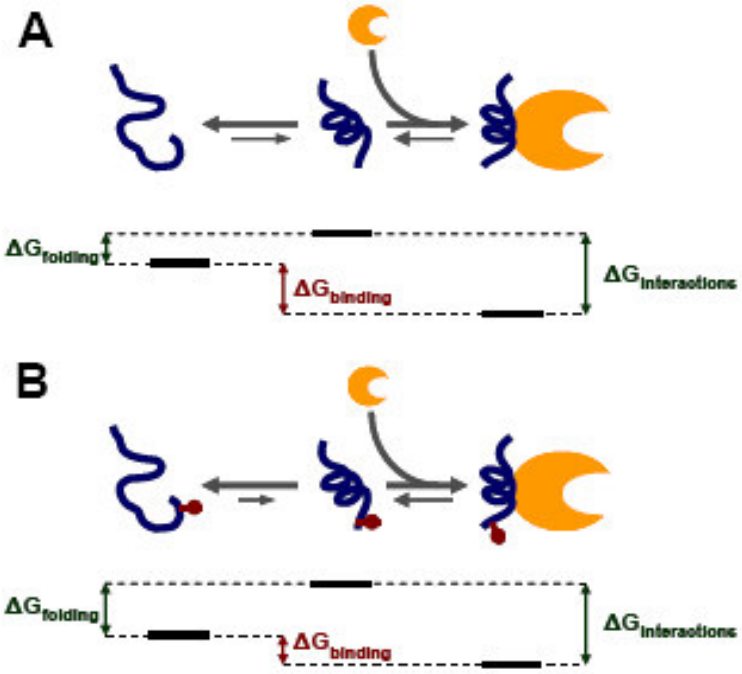

Figure 4.1 Model of disorder-order transition.

(A) Free energy diagram for the eIF4E binding domain of 4E-BP1 (in blue), showing the order-disorder transition of the non-complexed protein in solution on the left-hand-side and binding of the folded protein to eIF4E on the right-hand-side (eIF4E in orange). Suggested relationships between the respective ΔG values are shown (these are not to scale). (B) Free energy diagram for the phosphorylated form of the eIF4E binding domain of 4E-BP1, showing altered ΔG values.

Zor *et al* (2002) used similar techniques to investigate the roles of phosphorylation and secondary structure formation in the binding of the kinase inducible activation domain (KID) of CREB (cyclic AMP response element binding protein) to the KID binding domain (KIX) of CBP (CREB binding protein). In this case binding of unphosphorylated KID to KIX has a 2 order of magnitude lower affinity than phosphorylated, as shown by ITC. However phosphorylation of KID converts the low affinity complex into a specific high affinity complex by forming additional intermolecular interactions with KIX rather than influencing helical formation. The authors also generated mutations in one of the helices of phosphorylated KID (pKID) at solvent exposed positions, to either increase or decrease helical content, which was confirmed by CD. Helix destabilising mutations gave lower binding affinities and the authors conclude that the stability of this helix in pKID when bound to KIX is a major factor in high affinity binding.

Future Perspectives

Phosphorylation sites are often found in intrinsically unstructured regions (Iakoucheva *et al*, 2004) and this is the case with 4E-BP1. The C-terminal end of 4E-BP1 has a number of phosphorylation sites (Wang *et al*, 2003) and Molecular Dynamics simulations indicate that phosphorylation of 4E-BP1 can cause changes in the C-terminal region of the protein that influence binding (Tomoo *et al*, 2005). To investigate the influence of the other phosphorylation sites of 4E-BP1 on binding eIF4E, recombinant full length 4E-BP1 could be prepared, phosphorylated on each of the other sites, and used in ITC experiments titrated with eIF4E to see how much of a role each of the sites may play in the thermodynamics of binding, either individually or in combination. These results could further add to the SPR and

fluorescence data already performed by this group and others (Karim *et al*, 2001; Gingras *et al*, 1999).

ITC experiments with "stapled" peptides to hold the α-helical conformation would also give further evidence that the stability of the helix is important for tight binding. These peptides should give stronger binding affinities than the wild type peptide.

Other regions outside the eIF4E binding site of 4E-BP1 may also play an important role in the thermodynamics of binding. Further ITC experiments could be performed with the full length 4E-BP1, containing the same mutations as the peptides in this study, titrated with eIF4E. Comparison with the peptide could show any differences in binding between the two and may indicate how much influence the rest of the 4E-BP1 around the binding site has on its interaction with eIF4E.

We have performed a comprehensive biophysical analysis using a number of different techniques. ITC has been used to give binding affinities between peptides of 4E-BP1$_{51-67}$ and eIF4E and these provide information on specific residues in the eIF4E binding domain and how they influence the thermodynamics of binding. Also our NMR data gives further structural information on the influence of the met60 and arg63 residues and phosphorylation of 4E-BP1 and the changes occuring on binding eIF4E. This adds to the growing data on unstructured proteins and can give insight into the mechanisms employed by this group of proteins.

References

Abiko, F., Tomoo, K., Mizuno, A., Morino, S., Imataka, H. and Ishida, T. (2007) Binding preference of eIF4E for 4E-binding protein isoform and function of eIF4E N-terminal flexible region for interaction, studied by SPR analysis *Biochemical and Biophysical Research Communications*, **355**, 667-672

Algire, M. A. and Lorsch J. R. (2006) Where to begin? The mechanism of translation initiation codon selection in eukaryotes *Current Opinion in Chemical Biology*, **10**, 480-486

De Benedetti, A. and Graff, J. R. (2004) eIF4E expression and its role in malignancies and metastases *Oncogene*, **23**, 3189-3199

Duncan, R., Milburn, S. C. and Hershey, J. W. (1987) Regulated phosphorylation and low abundance of HeLa cell initiation factor eIF4F suggest a role in translational control *The Journal of Biological Chemistry*, **262**, 380-388

Dunker, A. K., Brown, C. J., Lawson, J. D., Iakoucheva, L. M. and Obradović, Z. (2002) Intrinsic disorder and protein function *Biochemistry*, **41**, 6573-6582

Dyson, H. J. and Wright, P. E. (2002) Coupling of folding and binding for unstructured proteins *Current Opinion in Structural Biology*, **12**, 54-60

Dyson, H. J. and Wright, P. E. (2005) Intrinsically unstructured proteins and their functions *Nature Reviews Molecular Cell Biology*, **6**, 197-208

Fletcher, C. M. and Wagner, G. (1998) The interaction of eIF4E with 4E-BP1 is an induced fit to a completely disordered protein *Protein Science,* **7**, 1639-1642

Fletcher, C. M. *et al* (1998) 4E binding proteins inhibit the translation factor eIF4E without folded structure *Biochemistry*, **37**, 9-15

Gingras, A.-C., Raught, B. and Sonenberg, N. (1999) eIF4 initiation factors: effectors of mRNA recruitment to ribosomes and regulators of translation *Annual Review of Biochemistry*, **68**, 913-963

Gingras, A.-C., Gygi, S. P., Raught, B., Polakiewicz, R. D., Abraham, R. T., Hoekstra, M. F., Aebersold, R. and Sonenberg, N. (1999) Regulation of 4E-BP1 phosphorylation: a novel two-step mechanism *Genes & Development*, **13**, 1422-1437

Gingras, A.-C. *et al* (2001) Hierarchical phosphorylation of the translational inhibitor 4E-BP1 *Genes & Development*, **15**, 2852-2864

Gross, J. D. *et al* (2003) Ribosome loading onto the mRNA cap is driven by conformational coupling between eIF4G and eIF4E *Cell*, **115**, 739-750

Grossman, A. D., Erickson, J. W. and Gross, C.A. (1984) The htpR gene product of *E. Coli* is a sigma factor for heat-shock promoters *Cell*, **38**, 383-90

Gunasekaran, K., Tsai, C. J., Kumar, S., Zanuy, D. and Nussinov, R. (2003) Extended disordered proteins: targeting function with less scaffold *Trends in Biochemical Sciences*, **28**, 81-85

Haghighat, A., Mader, S., Pause, A. and Sonenberg N. (1995) Repression of cap-dependent translation by 4E-binding protein 1: competition with p220 for binding to eukaryotic initiation factor 4E *The EMBO Journal*, **14**, 5701-5709

Hershey, P., McWhirter, S. M., Gross, J. D., Wagner, G., Alber, T. and Sachs, A. B. (1999) The cap binding protein eIF4E promotes folding of a functional domain of yeast translation initiation factor eIF4G1 *Journal of Biological Chemistry*, **274**, 21297-21304

Hinnebusch, A. G. (2006) eIF3: a versatile scaffold for translation initiation complexes *Trends in Biological Sciences*, **31**, 553-562

Hiremath, L. S., Webb, N. R., Rhoads, R. E. (1985) Immunological detection of the messenger RNA cap-binding protein *Journal of Biological Chemistry*, **260**, 7843-7849

Iakoucheva, L. M., Radivojac, P., Brown, C. J., O'Connor, T. R., Sikes, J. G., Obradovic, Z. and Dunker, A. K. (2004) The importance of intrinsic disorder for protein phosphorylation *Nucleic Acids Research*, **32**, 1037-1049

Karim, M. M., Hughes, J. M., Warwicker, J., Scheper, G. C., Proud, C. G. and McCarthy, J. E. (2001) A quantitative molecular model for modulation of mammalian translation by the eIF4E-binding protein 1 *Journal of Biological Chemistry*, **276**, 20750-20757

Lin, T.-A. *et al* (1994) PHAS-I as a link between mitogen-activated protein kinase and translation initiation *Science*, **266**, 653-656

Mader, S., Lee, H., Pause, A. and Sonenberg, N. (1995) The translation initiation factor eIF4E binds to a common motif shared by the translation factor eIF4γ and the translational repressors 4E-binding proteins *Molecular and Cellular Biology*, **15**, 4990-4997

Marcotrigiano, J., Gingras, A.-C., Sonenberg, N. and Burley, S. K. (1997) Co-crystal structure of the messenger RNA 5' cap-binding protein (eIF4E) bound to 7-methyl-GDP *Cell*, **89,** 951-961

Marcotrigiano, J., Gingras, A.-C., Sonenberg, N. and Burley, S. K. (1999) Cap-Dependent translation initiation in eukaryotes is regulated by a molecular mimic of eIF4G *Molecular Cell*, **3**, 707-716

Matsuo, H., Li, H., McGuire, A. M., Fletcher, C. M., Gingras, A.-C., Sonenberg, N. and Wagner, G. (1997) Structure of translation factor eIF4E bound to m7GDP and interaction with 4E-binding protein *Nature Structural Biology*, **4**, 717-724

Mitchell, S. F. and Lorsch, J. R. (2008) Should I stay or should I go? Eukaryotic translation initiation factors 1 and 1A control start codon recognition *Journal of Biological Chemistry*, **283**, 27345-27349

Mizuno, A., In, Y., Fujita, Y., Abiko, F., Miyagawa, H., Kitamura, K., Tomoo, K. and Ishida T. (2008) Importance of C-terminal flexible region of 4E-binding protein in binding with eukaryotic initiation factor 4E *FEBS Letters*, **582**, 3439-3444

Mothe-Satney, I., Yang, D., Fadden, P., Haystead, T. A. and Lawrence, J. C. Jr. (2000a) Multiple mechanisms control phosphorylation of PHAS-I in five (S/T)P sites that govern translational repression *Molecular and Cellular Biology*, **20**, 3558-3567

Mothe-Satney, I., Brunn, G. J., McMahon, L. P., Capaldo, C. T., Abraham, R. T. and Lawrence, J. C. Jr. (2000b) Mammalian target of rapamycin dependent phosphorylation of PHAS-I in four (S/T)P sites detected by phospho-specific antibodies *Journal of Biological Chemistry*, **275**, 33836-33843

Pause, A., Belsham, G. J., Gingras, A.-C., Donzé, O., Lin, T. A., Lawrence, J. C. Jr. and Sonenberg, N. (1994) Insulin-dependent stimulation of protein synthesis by phosphorylation of a regulator of 5'-cap function *Nature*, **371**, 762-767

Poulin, F., Gingras, A.-C., Olsen, H., Chevalier, S. and Sonenberg, N. (1998) 4E-BP3, a new member of the eukaryotic initiation factor 4E-binding protein family *Journal of Biological Chemistry*, **273**, 14002-14007

Ptushkina, M., von der Haar, T., Vasilescu, S., Frank, R., Birkenhäger, R. and McCarthy, J. E. (1998) Cooperative modulation by eIF4G of eIF4E binding to the mRNA 5'cap in yeast involves a site partially shared by p20 *The EMBO Journal,* **17**, 4798-4808

Ptushkina, M., von der Haar, T., Karim, M. M., Hughes, J. M. and McCarthy, J. E. (1999) Repressor binding to a dorsal regulatory site traps human eIF4E in a high cap-affinity state *The EMBO Journal*, **18**, 4068-4075

Raught, B. and Gingras, A.-C. (1999) eIF4E activity is regulated at multiple levels *The International Journal of Biochemistry & Cell Biology*, **31**, 43-57

Rohl, C. A., Chakrabartty, A. and Baldwin, R., L. (1996) Helix propagation and N-cap propensities of the amino acids measured in alanine-based peptides in 40 volume percent trifluoroethanol *Protein Science*, **5**, 2623-37

Scheper, G. C. and Proud, C. G. (2002) Does phosphorylation of the cap-binding protein eIF4E play a role in translation initiation? *European Journal of Biochemistry*, **269**, 5350-5359

Schneppe, B., Eichner, W. and McCarthy, J. E. (1994) Translational regulation of a recombinant operon containing human platelet-derived growth factor (PDGF)-encoding genes in *Escherichia coli*: genetic titration of the peptide chains of the heterodimer AB *Gene*, **143**, 201-209

Sonenberg, N., Morgan, M. A., Merrick, W. C. and Shatkin, A. J. (1978) A polypeptide in eukaryotic initiation factors that crosslinks specifically to the 5'-terminal cap in mRNA *Proc. Natl. Acad. Sci. USA*, **75**, 4843-4847

Sonenberg, N., Rupprecht, K. M., Hecht, S. M. and Shatkin, A. J. (1979) Eukaryotic mRNA cap binding protein: purification by affinity chromatography on sepharose-coupled m^7GDP *Proc. Natl. Acad. Sci. USA*, **76**, 4345-4349

Sonenberg, N. and Gingras, A.-C. (1998) The mRNA 5' cap-binding protein eIF4E and control of cell growth *Current Opinion in Cell Biology*, **10**, 268-275

Tomoo, K., Matsushita, Y., Fujisaki, H., Abiko, F., Shen, X., Taniguchi, T., Miyagawa, H., Kitamura, K., Miura, K. and Ishida, T. (2005) Structural basis for mRNA cap-binding regulation of eukaryotic initiation factor 4E by 4E-binding protein, studied by spectroscopic, X-ray crystal structural, and molecular dynamics simulation methods *Biochimica et Biophysica Acta*, **1753**, 191-208

Tomoo, K., Abiko, F., Miyagawa, H., Kitamura, K. and Ishida, T. (2006) Effect of N-terminal region of eIF4E and Ser65-phosphorylation of 4E-BP1 on interaction between eIF4E and 4E-BP1 fragment peptide *Journal of Biochemistry*, **140**, 237-246

Tompa, P. (2002) Intrinsically unstructured proteins *Trends in Biochemical Sciences*, **27**, 527-533

Tsukiyama-Kohara, K., Vidal, S. M., Gingras, A.-C, Glover, T. W., Hanash, S. M., Heng, H. and Sonenberg N. (1996) Tissue distribution, genomic structure, and chromosome mapping of mouse and human eukaryotic initiation factor 4E-binding proteins 1 and 2 *Genomics*, **38**, 353-363

Uversky, V. N., Gillespie, J. R. and Fink, A. L. (2000) Why are "natively unfolded" proteins unstructured under physiologic conditions? *Proteins: Structure, Function and Genetics*, **41**, 415-427

Uversky, V. N. (2002) Natively unfolded proteins: A point were biology waits for physics *Protein Science*, **11**, 739-756

Volpon, L., Osborne, M. J., Topisirovic, I., Siddiqui, N. and Borden, K. L. (2006) Cap-free structure of eIF4E suggests a basis for conformational regulation by its ligands *The EMBO Journal,* **25**, 5138-5149

Volpon, L., Osborne, M. J., Capul, A. A., de la Torre, J. C. and Borden, K. L. (2010) Structural characterisation of the Z RING-eIF4E complex reveals a distinct mode of control for eIF4E *Proc. Natl. Acad. Sci. USA*, **23**, 5441-5446

von der Haar, T., Gross, J. D., Wagner, G. and McCarthy, J. E. (2004) The mRNA cap binding protein eIF4E in post transcriptional gene expression *Nature Structural & Molecular Biology*, **11**, 503-511

Wang, X. *et al* (2003) The C terminus of initiation factor 4E-binding protein 1 contains multiple regulatory features that influence its function and phosphorylation *Molecular and Cellular Biology,* **23**, 1546-1557

Wright, P. E. and Dyson H. J. (1999) Intrinsically unstructured proteins: reassessing the protein structure-function paradigm *Journal of Molecular Biology*, **293**, 321-331

Zor, T., Mayr, B. M., Dyson, H. J., Montminy, M. R. and Wright, P. E. (2002) Roles of phosphorylation and helix propensity in the binding of the KIX domain of CREB-binding protein by constitutive (c-Myb) and inducible (CREB) activators *Journal of Biological Chemistry*, **277**, 42241-42248